THE PLUTONIC-DYKE SYSTEM AND HOST LIGURIAN SUCCESSIONS OF THE ISLAND OF MONTECRISTO (TUSCAN ARCHIPELAGO, ITALY): NEW STRATIGRAPHIC, PETROGRAPHIC AND STRUCTURAL DATA

Riccardo Giusti*,**, Giulio Colombo**, Enrico Pandeli**,°,✉, Franco Marco Elter***, Martina Casalini** and **Letizia Orti****

   * *The National Research Council of Italy - Bioeconomy Institute (CNR-IBE), Florence, Italy.*
  ** *Department of Earth Sciences, University of Florence, Italy.*
*** *DISTAV, Dipartimento di Scienze della Terra dell'Ambiente e della Vita, University of Genoa, Italy.*
   ° *National Researches Council-Geosciences and Earth Resources Institute (CNR-IGG, Pisa) -Florence section, Italy.*
  ✉ *Corresponding author, email: enrico.pandeli@unifi.it*

ABSTRACT

To improve the geological knowledge of the poorly studied and scarcely accessible Island of Montecristo (Tuscan Archipelago), the Authors performed 1:5000 geological survey, meso- and microstructural study and petrographic analyses on the Messinian pluton, on the associated dyke/vein network and on the remnants of the hornfels cover occurring along the western and southern coasts. The results of this study allow: a) to define a complex system of dykes and hydrothermal veins crossing the pluton and its hornfels. b) to directly correlate the Montecristo hornfels rocks (here grouped in the "Cala S. Maria-Cala dei Ladri Unit") with the contact metamorphic aureole of the Monte Capanne pluton of the Elba Island (i.e., the Punta Polveraia-Fetovaia Unit). The Cala S. Maria-Cala dei Ladri Unit is mainly composed of alternating metapelites and metasandstones (whose protolith is likely the Quartzarenitic Member of the Palombini Shales and/or the Val Lavagna Shales of Early-Late Cretaceous age) and of minor metaophiolitic rocks; metaserpentinites were also mapped for the first time. c) to recognize low-medium grade hornfels in the remnants of the contact metamorphic aureole and the ubiquitous presence of basal cataclastic horizons, testifying a role of "roof pendant" plates for the Cala S. Maria-Cala dei Ladri Unit outcrops. d) to reconstruct a complex structural evolution for the emplacement of the pluton and for its contact metamorphic aureole. This evolution started with ductile events, i.e., formation of mylonite in the granitoids and of a pervasive S_1 schistosity in the hornfels, which was likely related to flattening processes occurred during the balooning of the magmatic body, followed by ductile D_2 folding with the detachment of the recrystallized Ligurian covers due to the rise of the partially cooled pluton, and then by a series of jointing/faulting events, whose lineaments were used as pathways for the intrusion of the different dykes and hydrothermal veins; finally, a NW-SE striking transtensive sinistral shear zone (Cala Maestra-Cala Corfù Fracture Zone) with an about ENE-WSW directed σ_1 originated in the south/south-western part of the island. This shear zone represents one of the few witness of regional transcurrent structures in the Tuscan Archipelago and was likely active also during the emplacement of the plutonic body.

INTRODUCTION

The island of Montecristo, about 10 km² wide, steeply emerges up to 645 m from the Northern Tyrrhenian Sea. It is located in the southernmost part of the Tuscan Archipelago (latitude 42°19'51", longitude 10°18'36") about 40 km south of the Elba island and more than 60 km from the Italian and the Corsica coasts (Fig. 1). Its geographical location makes Montecristo one of the most isolated, impervious and naturalistically intact peculiar ecosystem in the Mediterranean area. It is protected as Biogenetic Natural Reserve (since 1971) within the Tuscan Archipelago National Park which strongly limits the access.

From a geological point of view, the Montecristo island consists of a Late Miocene monzogranitic pluton and dike network with a few and scattered remnants of its contact metamorphic aureole (Innocenti et al., 1997; Rocchi et al., 2003a and references therein) (Fig. 2a, b and c).

The geological literature of the island is scarce. Smith and Warington (1841) described for the first time the magmatic and metamorphic rocks of the island, followed by Giuli (1843), Pareto (1844), D'Anchiardi (1872), Jervis (1874) and Ugolini (1909). Roster (1876), Millosevich (1912) and Palache et al. (1951) characterized its uranium (metazeunerite)-bearing pegmatites. Mittempergher (1954) carried out a systematic geological study (including a geological map) and petrographic analyses of the Montecristo granitoid, of the dike network and of the hornfelses ("Schists").

In the last decades, Ferrara and Tonarini (1985), Innocenti et al. (1997) and Rocchi et al. (2003a) investigated the magmatic and structural features of the island (Fig. 2c), the cooling age (7.1 Ma, using Rb-Sr whole-rock-biotite radiometric method) and the emplacement of the pluton, and, to minor extent, the nature of the contact metamorphic host rocks, whose protoliths (gabbro and sedimentary rocks) were attributed to the oceanic internal Ligurian realm.

Other Authors (e.g., Poli et al., 1989; Poli and Peccerillo, 2016) focused on igneous petrology, discussing the role of Montecristo pluton within the magmatic frame of the Northern Apennines.

Anyway, few data are currently available for the metamorphic rocks of the aureole (Mittempergher, 1954; Innocenti et al., 1997) due to the scarcity of the outcrops, hardly accessible. Their detailed study is fundamental not only to define features and deformation-metamorphic evolution of the contact aureole, but also to deeply know the dynamics of the pluton emplacement as already defined for the granitoid plutons of the Elba Island (e.g., Porto Azzurro pluton in Garfagnoli et al., 2005, Caggianelli et al., 2018 and Spiess et al., 2021; Monte Capanne pluton in Rossetti et al., 2007 and Pandeli et al., 2018 and references therein).

The present paper aims to define in detail the geological frame of the Montecristo Island and reconstruct the deformation and metamorphic stages of the geological units, occurred
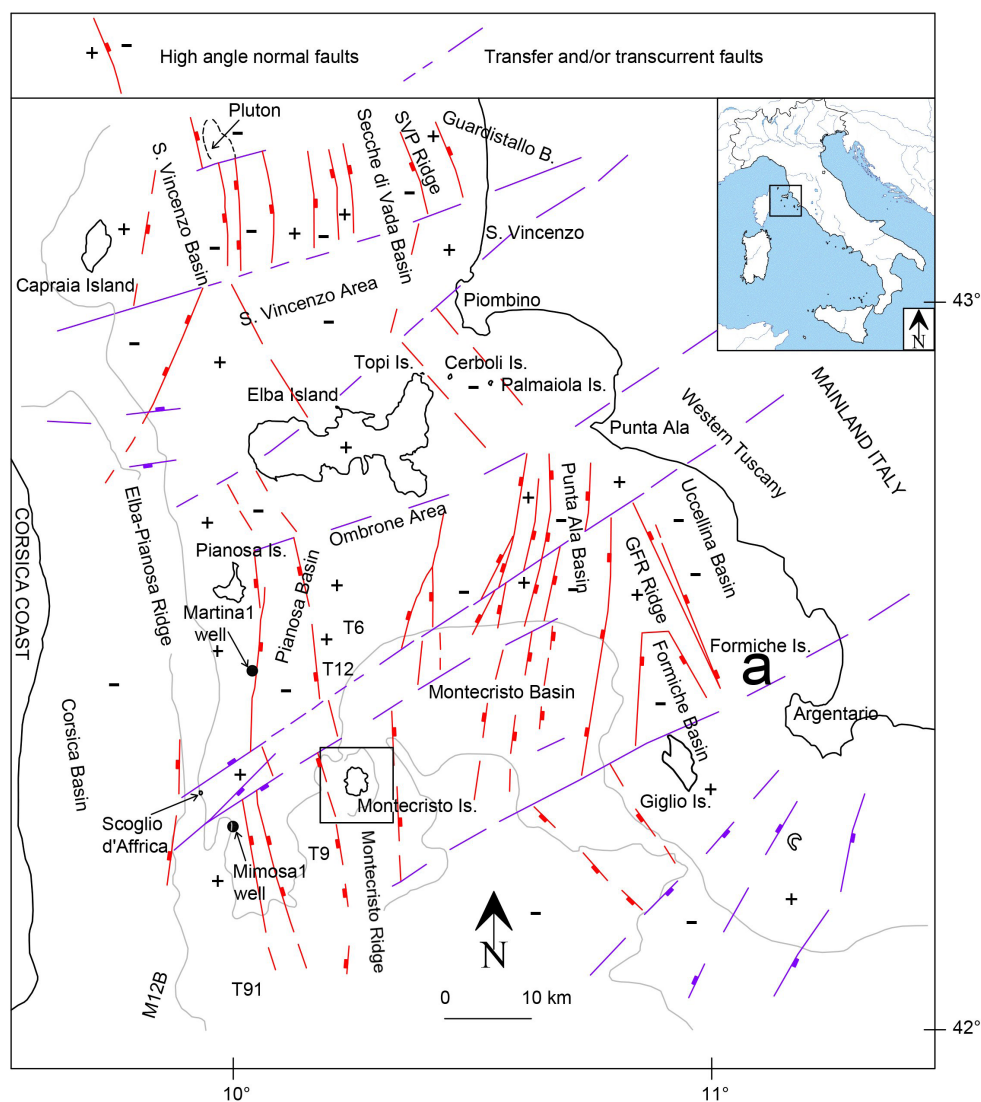
Fig. 1 - Structural sketch of the Northern Tyrrhenian Sea (modified from Bartole, 1994 and Cornamusini and Pascucci, 2014) and location of the Montecristo Island. The reader is referred to the PDF version of the article for a colour version.

during and after the emplacement of the pluton, through a multidisciplinary study including: i) geological mapping, ii) meso- and micro-structural studies of the outcrops and iii) petrographic and iv) X-ray mineralogical analyses of the lithotypes.

GEOLOGICAL FRAMEWORK

The genesis and emplacement of the Montecristo pluton are strictly connected to the lithosphere delamination processes of the inner part of the Adria plate,-the Northern Apennines chain-, made up of oceanic to transitional (Ligurian and sub-Ligurian, respectively), and continental (Tuscan and Umbrian-Marchean) nappes. These processes took place during post-collisional Neogene extensional phases (Bartole, 1995; Jolivet et al., 1998; Doglioni et al., 1999; Mauffret and Contrucci, 1999; Carmignani et al., 2001; Principi et al., 2015 and references therein) that allowed thinning of the lithosphere and ascent of the hot asthenosphere in an extensional setting. The back-arc propagated eastward progressively from the Northern Tyrrhenian Sea to the Apennine continental hinterland during the Late Miocene-Quaternary times and produced typical horst and graben structures at regional scale (Zitellini et al., 1986; Sartori et al., 1989; Bartole et al, 1991; Patacca et al., 1993; Bartole, 1995; Bortolotti et

al., 2001; Martini and Sagri, 1993; Cornamusini & Pascucci, 2014) (Fig. 1). The lithosphere extension was accompanied by diachronous anatectic magmatism of the so-called Late Miocene-Quaternary Tuscan Magmatic Province (Marinelli, 1967; Innocenti et al., 1992; Serri et al., 1993; Peccerillo, 2005). Anyway, the anatectic nature of the Tuscan magmatism was reconsidered because this Province includes magmatic bodies characterized by different sources and petrogenetic signature with mingling and mixing processes of basic mantle-derived and anatectic crustal magmas (Serri et al., 2001; Peccerillo, 2005; Conticelli et al., 2015 and references therein).

The Messinian Montecristo monzogranite forms more than 95% of the rocks of the island and shows a sub-circular shape with a diameter of about 4 km (Fig. 2c). This peraluminous magmatic body, transitional sub-alkaline/alkaline in composition (Rocchi et al., 2003a), is located on the western border of the Montecristo ridge (Fig. 1) and was emplaced at relatively shallow depth in the highest portion of the collapsed Apenninic accretionary wedge (i.e., in the Ligurian nappes), similarly to the Mt. Capanne pluton in Elba Island (Dini et al., 2002; Westerman et al., 2004; Bortolotti et al., 2001; Pandeli et al., 2018). The geochemical features of the pluton show that it has a dominant anatectic origin from partial melting of lower crustal metapelites (as inferred from high $^{87}Sr/^{86}Sr$ and the low $^{143}Nd/^{144}Nd$ ratios in Innocenti et al., 1997).

Compared to the other plutonic bodies of the Tuscan Archipelago and of the mainland (e.g., Mt. Capanne and Porto Azzurro plutons in the Elba Island; Gavorrano pluton and Campiglia pluton in Maritime Tuscany), the contact metamorphic aureole of the Montecristo granitoid is poorly preserved (Innocenti et al., 1997; Rocchi et al., 2003a) (Fig. 2). Only a dozen of small and scattered outcrops of hornfels are present in the southern (Cale Gemelle, Cala dei Ladri, Punta Rossa and Cala Corfù) and in the western parts (promontory between Cala S. Maria and Cala Mendolina) of the island. A preserved more continuous contact of the pluton with the surrounding contact aureole rocks can be identified offshore on a morphological slope break at about 100 m below the sea level (Innocenti et al., 1997). Various joints and fault systems, frequently intruded by magmatic dikes and pegmatitic to hydrothermal veins, crosscut the pluton. In particular, these brittle structures concentrate along the ~ 1 km-thick Cala Maestra-Cala Corfù Fracture Zone (MCFZ in Innocenti et al, 1997) in the southern part of the island (Fig. 2c).

MATERIALS AND METHODS

The Authors present here a 1:5000 scale geological map (topographic base from 1:25000 sheet MON and from 1:10000 sheet n. 328 - Isola di Montecristo of Regione Toscana) and a mesoscopic structural survey on the outcrops of the hornfels and their magmatic surroundings in the southern and western part of the island. Microstructural, petrographic and X-ray mineralogical analyses were also carried outcarried out on forty seven representative samples from both magmatic/hydrothermal and hornfels rocks. The An mol% content of the plagioclases was defined through petrographic (e.g., Michel-Levy method, Carlsbad-Albite method) and X-ray analyses. X-ray diffraction (XRD) analyses. XRD analyses were performed in the laboratories of the Department of Earth Sciences in the University of Florence, utilizing a Philips PW 1050/37 diffractometer with a Philips X'Pert PRO data acquisition and interpretation system, operating at 40 kV-20 mA, with a Cu anode, a graphite monochromator and with 2°/min goniometry speed in a scanning range between 5°-70°θ. Mineral abbreviations used in the text and in Tables 1-2-3 are from Whitney and Evans (2010).

LITHOLOGY, PETROGRAPHY AND STRUCTURAL FEATURES

The data obtained from the study of the igneous and contact metamorphic rocks are shown in the following paragraphs and in the geological maps of Fig. 2a and b. The petrographic data of the hornfels are summarized in Tables 1-2-3. Mineral abbreviations are from Whitney and Evans (2010).
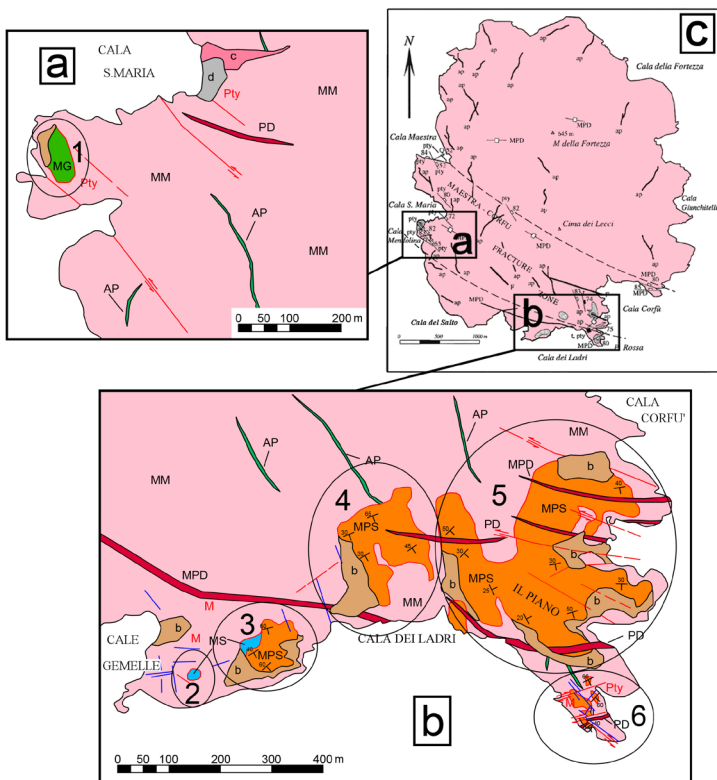

Fig. 2 - Geological sketch maps of the studied hornfels outcrops in the Island of Montecristo (a and b). The outcrops are numbered as in the text. c) Geological sketch of the whole island after Innocenti et al. (1997): ap=aplite dikes, pty=pseudotachylites, t=tourmaline-coated joints, Q=quartz lineations, MPD=Montecristo porphyritic dikes.

Table 1 - Petrographic-mineralogical features of the Cala S. Maria-Cala dei Ladri Unit rocks: metagabbros.

Metagabbros				
Contact metamorphism	Textures	Mineralogic associations	Veins	Outcrops
Low- grade	Coarse grained granoblastic/porphyro--clastic to cataclastic	Tr/Act (after Cpx) + +Plo (to Pla) ± Tlc ± Chl Accessories: Ep, Fe - Ox/Hydrox, Tur Porphyroclasts: - Cpx mostly transformed into Tr - Zoned Pl (Pla to Pll core, Plo (to Pla) rim), often cataclastic, with Act± Chl veins	Fe Ox/Hydrox+ +Act ± Tur + +Py ± Ep; Chl	1 (northern portion)
Transition low- to medium grade	Layered texture: alternating fine-grained cataclastic-mylonitic to nematoblastic	Tr/Act + Plo to Pla± ±Qtz ± Bt + Spn (± Cpx) Porphyroclasts: idem Accessories: Ep, Fe-Ox/Hydrox, Tur, Py S1= Tr + Plo to Pla± Qtz ± Chl ± Bt + Spn	Qtz + Cpx + +Pla to Pll (also deformed by D2) Tr/Act + Py; Qtz + Py; Fe-Ox/Hydrox	1 (southern portion)
	Coarse-grained granoblastic texture	Cpx (neo-formed diopside) + Pla to Pll± Qtz Accessories: Ep, Fe-Ox/Hydrox-	Deformed bands of Cpx + Pla to Pll lens and veins of Cpx +Pll to Plb and of Qtz	

Mineral abbreviations from Whitney and Evans (2010). For Pl: Plo = oligoclasic plagioclase, Pla = andesinic plagioclase, Pll = labradoritic plagioclase, Plb = bytownitic plagioclase (the detailed data about the mol% An are reported in the text)

Table 2 - Petrographic-mineralogical features of the Cala S. Maria-Cala dei Ladri Unit rocks: metaserpentinites

Metaserpentinites				
Contact metamorphism	Textures	Mineralogic associations	Veins	Outcrops
Transition low- to medium grade	Medium-grained nematoblastic/ porphyroclastic to, locally, cataclastic-mylonitic	Tr (or locally Hbl±Grt) +Py+ Fe Ox/Hydrox Cpx (± rare OPx) porpyroclasts mostly transformed into Tr ± Qtz Accessories: Ep, Zrn, Aln, Spn (± Rt) S1= Tr + Fe Ox/Hydrox ± Qtz	Chl	2, 3

Mineral abbreviations as in Table 1.

Table 3 - Petrographic-mineralogical features of the Cala S. Maria-Cala dei Ladri Unit rocks: metapelites and quartzitic metasandstones

Contact metamorphism grade	Textures	Mineralogic associations	Veins	Outcrops
Very low grade	Fine- to medium-grained, moderately sorted psammitic to blastopsammitic (weakly recrystallized sandstone)	Angular to sub-angular, rarely sub-rounded Qtz grains in a Bt + Qtz + Fe-Ox/Hydrox- ± Ms matrix. Rare Plo. Accessories: Zr, Fe Ox/Idrox	Fe Ox/Hydrox	upper part of 4, 5 and 6
Low grade	Fine grained lepidoblastic to fine-grained blastopsammitic (metapelite)	Bt + Qtz ± Ms ± Fe-Ox/Hydrox Local spreads of Tur	Fe Ox/Hydrox +Tur Ep + Ax(Fe) +Adl + Qtz Qtz + Adl	3, 4, 5, 6
Low grade	Fine grained granoblastic, blastopsammitic, porphyroblastic to foliated (quartzite)	Qtz + Bt ± Ms + Fe-Ox/Hydrox; Rare Plo-Pla. S1= Bt + Qtz ± Ms ± Fe-Ox/Hydrox Accessories: Zr, Ep, Fe-Ox/Idrox-	Cpx + Pla to Pll +Qtz± Rt Qtz + Px Ep + Ax(Fe) +Adl + Qtz Ep + Ax(Fe)	3, 4, 5, 6
Low grade	Granoblastic (chloritic marble and calcschists) (after Mittempergher, 1954)	Cal+ Chl ± Qtz ± Ep ±Fe-Ox/Hydrox ± Py		3,4,5
Transition low Grade to medium grade and medium grade	Fine-medium grained, granoblastic to coarse-grained granoblastic (garnet-rich skarn)	Bt + Ms + Qtz ± Pla to Pll± Cpx ± Spn Porphyroclasts of Cpx and glomero-porphyroclasts of Cpx + Pla to Pll ±Spn Skarn levels: (Grs-Adr) ± Tr or Grt ± Cpx ± Qtz ±Bt ± Pll ± Fe Ox/Hydrox Accessories: Zr, Tur, Ap, Ep, Fe Ox/Hydrox	Ep; Ep + Adl; Tr/Act+ Spn Bands and veins of Cpx + Pll ±Spn Veins of Cpx +Pll to Plb±Spn ±Grt± Wo (in the salband)	3, 4, 5, 6

Mineral abbreviations as in Table 1.

LITHOLOGY AND PETROGRAPHY OF THE MAGMATIC ROCKS

The monzogranitic pluton

The Montecristo Monzogranite contains variable amounts of Kfs, Qtz and Pl phenocrysts in a granular groundmass made up of the same minerals and Bt (8-12% according to Innocenti et al., 1997) (Fig. 3a). The Kfs and Qtz phenocrysts reach sizes up to 13 cm and 3 cm, respectively, whereas Pl is up to 1 cm. Pl- and Bt-rich mafic microgranular enclaves (MME in Fig. 3b and c), monzogranitic to granodioritic/monzodioritic in composition (Innocenti et al., 1997), are a common occurrence in the granitoid body throughout the whole island. The monzogranitic pluton shows two main textural facies: i) a dominant, light-colored facies (MM$_1$ in Fig. 3a), with a lower Bt and a high Kfs phenocrysts content and ii) a dark-colored facies

(MM$_2$ in Fig. 3a), which is more enriched in Bt and in mafic enclaves. The Kfs phenocrysts concentration is locally high, reaching also cumulitic abundances (e.g., up to 70% in volume at Marina of Cala Maestra and Punta Rossa). The isorientation of the Kfs phenocrysts due to magmatic flow processes is visible at places (e.g., Punta Rossa) producing a primary magmatic foliation (Fig. 3d). Diacronous fracture sets and shear horizons, both with a main NW-SE and a secondary NE-SW strike, are present within the plutonic body in the different parts of the island, but particularly in its southern area along the Cala Maestra-Cala Corfù Fracture Zone. Here, mylonites, protomylonites and pseudotachilites can be distinguished too (see later).

From a petrographic point of view, the Kfs phenocrysts are frequently Carlsbad twinned Or crystals with micropertitic exsolutions laminae. Qtz phenocrysts contain blue Tur, Zrn and anhedral Bt inclusions whereas the Pl phenocrysts are acidic
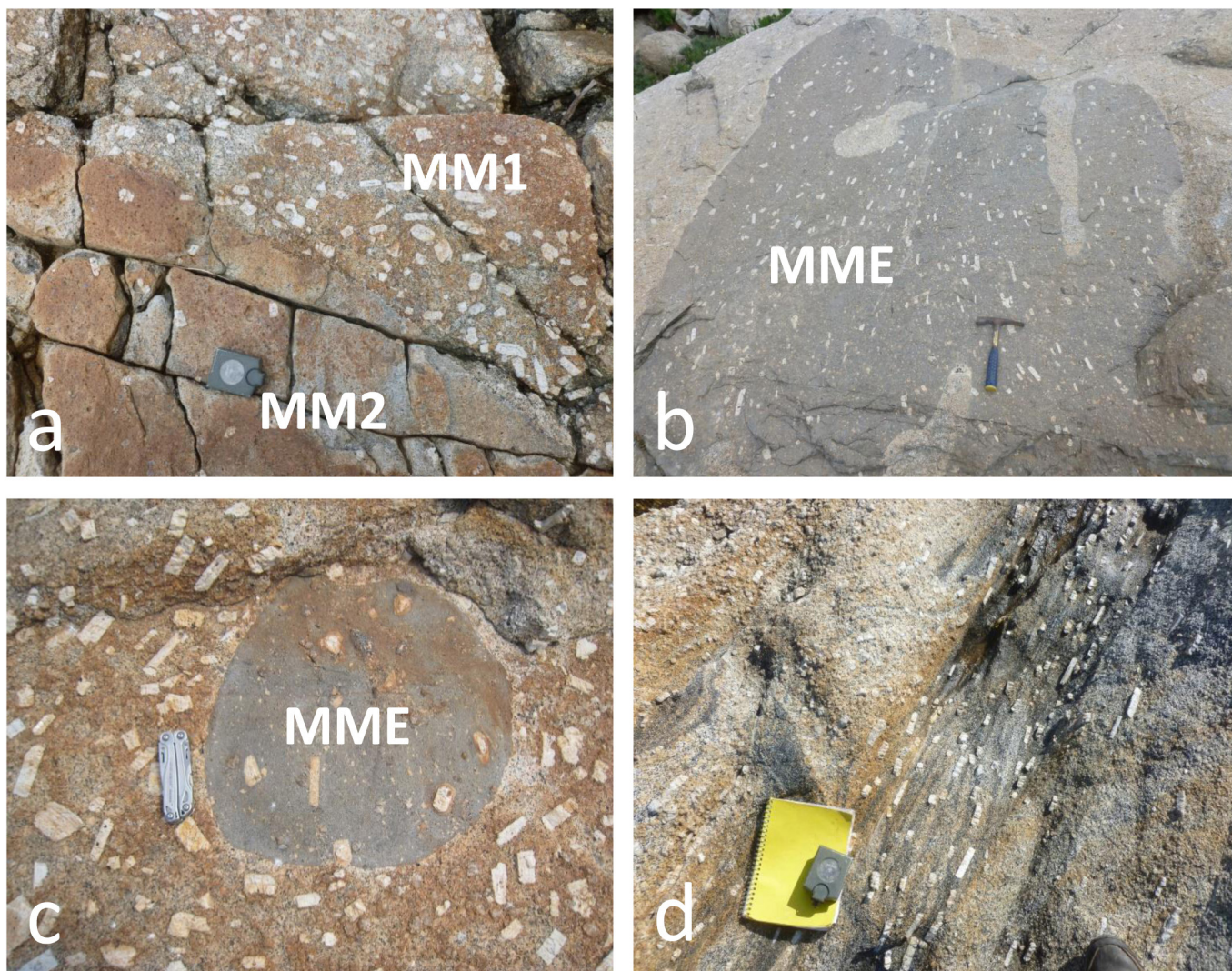
Fig. 3 - Textural features of the Montecristo monzogranite: a) K-feldspar phenocryst-rich (MM1) and -phenocryst-poor (MM2) facies in the Monzogranite at Cala Maestra; b) Irregular, metre-sized mafic enclave (MME) in the Monzogranite at Cala Maestra; c) Decimetre-sized spherical mafic enclave (MME) in the Monzogranite at Cala Maestra; d) Magmatic flow in the Monzogranite at Punta Rossa.

to intermediate (An 17 to 35 mol %) and frequently normally zoned and/or twinned. The groundmass shows a monzogranitic composition (42% Plg, 27% Qtz, 22% Kfs, 9% Bt on the average in Mittempergher, 1954) according to IUGS (International Union of Geological Sciences) classification, while Tur, Ap, Zrn and often altered Ilm (leucoxene) represent the accessory minerals; sericitized Crd is locally present.

Dykes and hydrothermal veins

Several types of dikes and veins were recognized in addition to the aplitic and porphyritic dikes s.l. described by previous Authors (Mittempergher, 1954; Innocenti et al., 1997). The dikes cross-cut the monzogranitic body and, some of them, are also hosted by the hornfels. The intrusion sequence of these bodies was inferred through their cross-cutting relationships both with the pluton and its metamorphic contact aureole rocks (Fig. 4).

We focused our investigation along the Cala Maestra-Cala Corfù Fracture Zone where all these magmatic and hydrothermal bodies are widely present. They are described below according to their relative chronology of emplacement (from the older, see Fig. 4).

Aplitic dikes

The Aplitic dykes (named "*ap*" in Innocenti et al., 1997; see Fig. 2c) are the most common dikes in the whole island, mainly in the south-western part of the pluton (e.g. along the Cala Maestra-Cala Corfù Fracture Zone) and in the areas characterized by lower topographic elevations (e.g., Cala del Salto, in the SW coast, see Fig. 2). They intrude the Monzogranite (Fig. 5a), but they were never found in the hornfels outcrops. These aplites are white to light gray in colour and with lengths between 5-25 m and thickness variable from 10 to 30 cm.

The Aplitic dikes are characterized by an overall fine-grained granular texture, but they locally include small phenocrysts of Qtz, Pl (oligoclase), Kfs and schorlitic Tur. The groundmass shows a typical aplitic mineralogical composition (31% Qtz, 27% Plg, 40% Kfs, 2% Tur). Minor Ms crystals are present, Bt is instead rare.

Qtz and Tur veins

These veins were distinguished for the first time during this study. They always crosscut the Aplitic dikes in Cala Maestra-Cala Corfù Fracture Zone (particularly in the Punta Rossa area) (Fig. 5a) and the Monzogranite (Fig. 5a and b), but not the hornfels. The Qtz and Tur veins are black to dark

grey in colour, thin (2-20 cm) and continuous for tens of meters (up to about 30 m in length). They are characterized by an almost homogeneous holocrystalline granular texture, with some scattered Tur phenocrysts (up to 7 cm), frequently arranged in fibrous aggregates. The groundmass is almost completely constituted by Qtz (60 %) and schorlitic Tur (about 40 %), with minor Ms (less than 0.5 %).

Tur-bearing porphyritic dikes and veins

They, not reported so far, constitute small bodies cropping out only in the Cala Maestra-Cala Corfù Fracture Zone and, in particular, close to the main shear zones (e.g., in the Cale Gemelle and *Punta Rossa* areas) and never above 200 m a.s.l. Their length does not exceed 40 m and the thickness generally ranges between 10 and 80 cm (max 1.3 m). Two types are distinguishable on the basis of the color index, i.e., a dark gray one, containing Bt, and a lighter one, without Bt (TPDb and TPDnb, respectively, in Fig. 5c and d). The TPDb dikes cross the TPDnb light ones (Figs. 4 and 5c) and both cut the Monzogranite and the Aplitic dikes (Fig. 5d), the Qtz and Tur veins veins and the host metamorphic rocks (Fig. 5c).

The TPDb dikes and veins are characterized by a porphyritic holocrystalline texture, with Kfs (up to 12 cm) and Bt (up to 4%) + Qtz + Kfs and Pl subhedral glomeroporphyritic aggregates. Colour index also spatially varies in function of density of Kfs, especially in the Punta Rossa area, where these veins can be paler than the monzogranitic pluton. Pl are distinctly sodic (An 15-25%). Qtz, Kfs, Pl and greenish-yellow microcrystals of schorlitic Tur (up to 4%) ± Bt constitute the medium-grained groundmass. Felsic mineral mode (55% Kfs, 35% Qtz, 10% Pl) point to a leucogranitic/granitic composition for dark grey tourmalinic porphyritic veins.

The TPDnb dikes and veins exhibit a microcrystalline granular to porphyritic texture, absence of Bt and scarcity of Kfs (up to 9 cm). Qtz (40%) and Kfs (50%) represent most of the mineral assemblage, while Pl (10%) and microcrystalline Tur (2%) are significantly lower; therefore, they can be classified as aplites.

Porphyritic dikes

The Porphyritic dikes (*p, gr* or MPD in Innocenti et al., 1997; see Fig. 2c), mostly present along the Cala Maestra-Cala Corfù Fracture Zone (particularly in the Punta Rossa area), intrude all the magmatic and hydrothermal bodies as well as the metamorphic rocks of the aureole (see Fig. 4). They are whitish to gray-greenish (Fig. 5e), but brown-reddish when altered. Qtz-filled orthogonal veins frequently cross the Porphyritic dikes, so that the different weathering behaviour of these two lithotypes produce peculiar alveolar "honeycomb" erosional forms. These dikes can have different lenghts: the longest dike is up to 1 km and 9 m - thick in the southernmost part of Cala dei Ladri, but the length generally ranges between 50 m and 150 m or less (locally 1 m). These leucogranitic dikes are characterized by a peculiar porphyritic holocrystalline texture, with phenocrysts of Qtz (up to 2 cm in size, sometimes cataclastic) and subordinately of feldspars (Carlsbad-twinned Kfs and polysynthetic twinned Pl with An 15-34 mol%, up to 10 cm in size) that
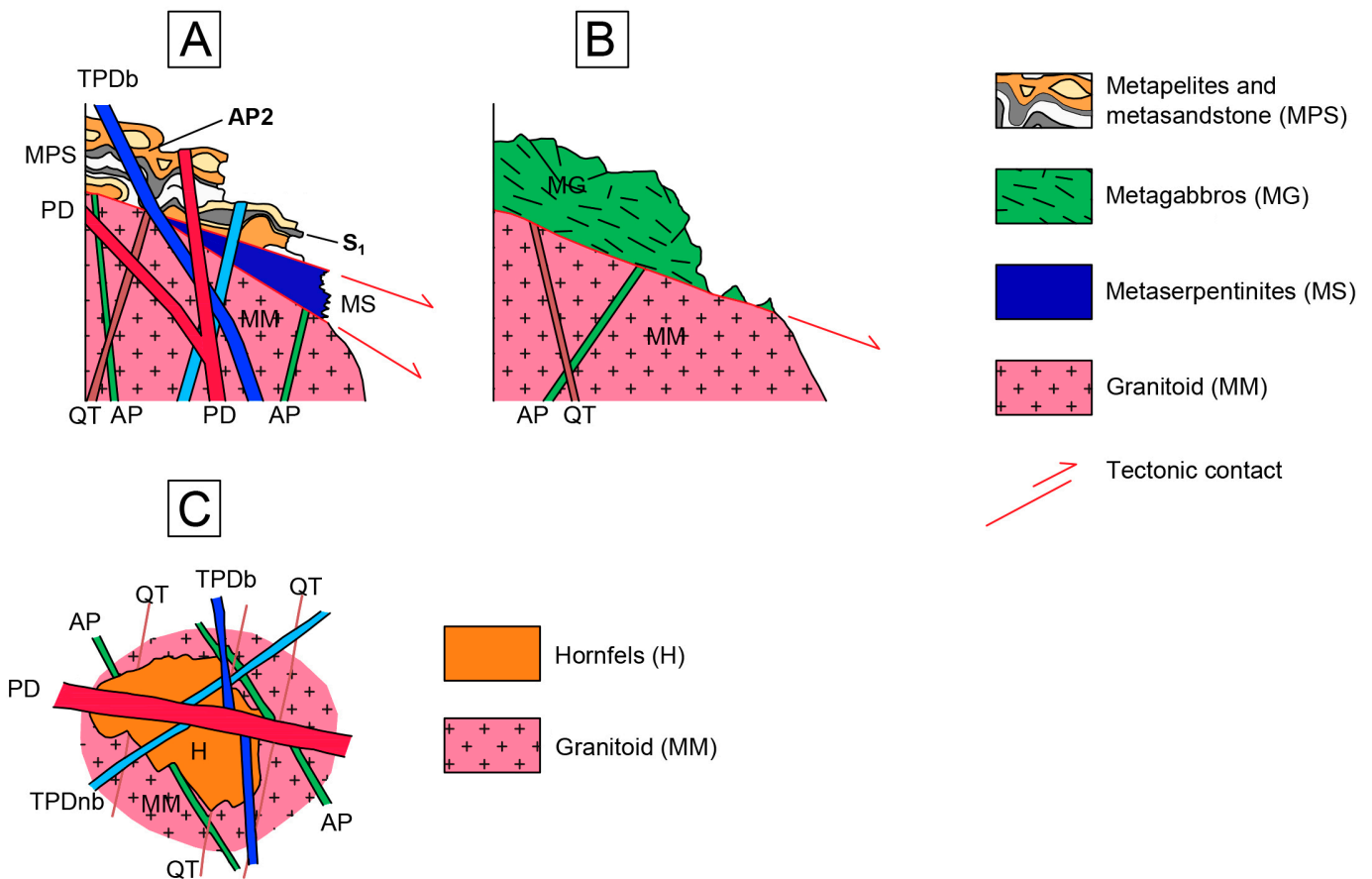

Fig. 4 - Relationships between the different magmatic dikes/hydrothermal veins and structures within the Monzogranite and hornfelses in the Outcrops 2 and 3 (A) and in the Outcrop 1 (B). General sketch of the crosscutting relations of magmatic dikes/hydrothermal veins with the monzogranite and hornfels in (C), acronyms: AP = Aplitic dikes, QT = Qtz and Tur veins, TPD (Tur-bearing porphyritic dikes and veins; TPDb with Bt, TPDnb without Bt), PD = Porphyritic dikes. In the hornfels S_1 = main foliation, AP2 = Axial plane of the D_2 folds.
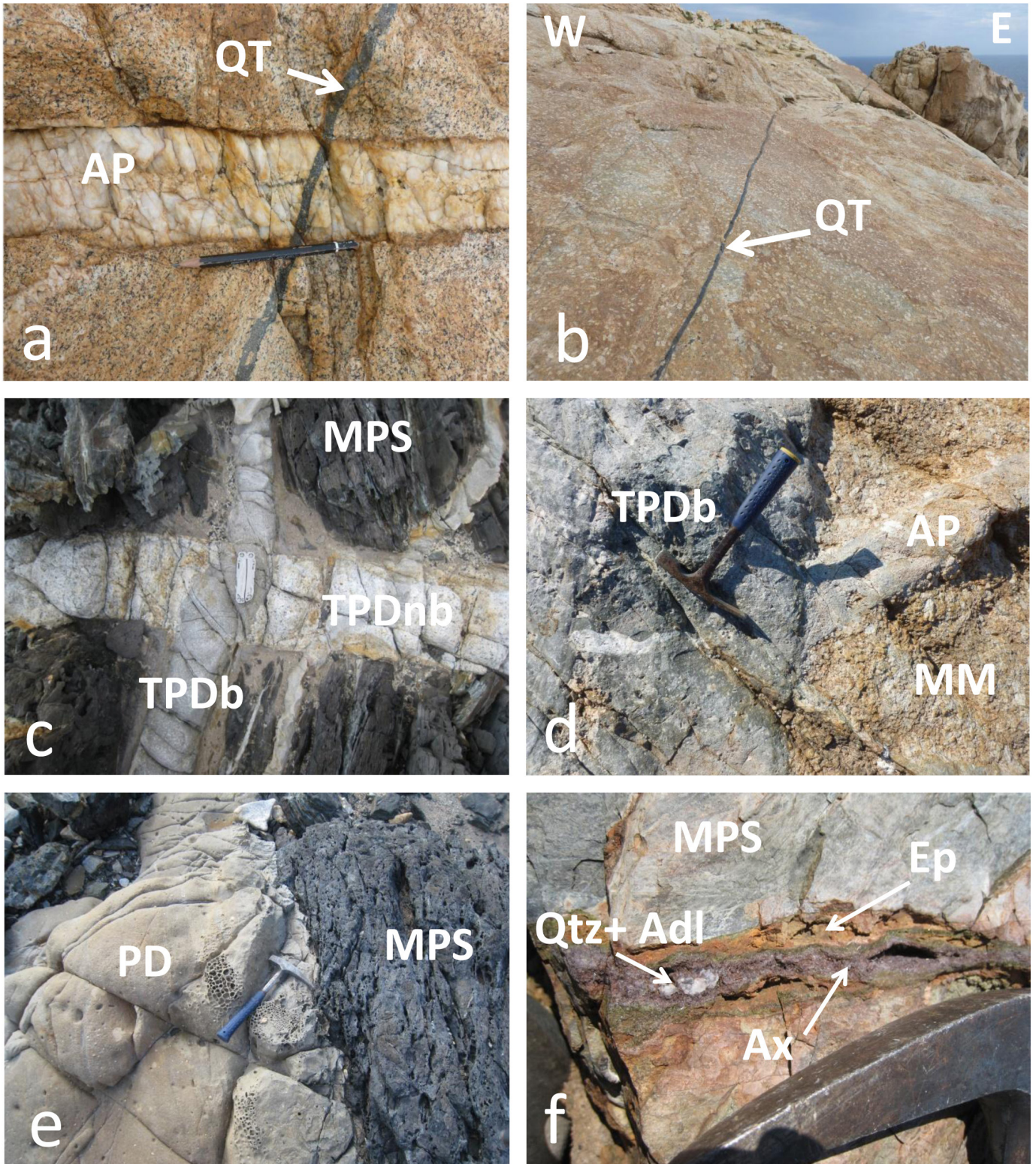
Fig. 5 - Features of the magmatic dikes and veins: a) Quartz-tourmaline vein (QT) cutting an aplitic dike (AP) and host Monzogranite at Punta Rossa; b) Outcrop of the Monzogranite cut by a Quartz-tourmaline vein (QT) at Il Piano locality; c) Bt-rich Tur porphyritic dike (TPDb) cutting Bt-poor Tur porphyritic dike (TPDnb) within the Metapelites and metasandstones (MPS) hornfels at Punta Rossa; d) Bt-rich Tur porphyritic dike (TPDb) cutting the Monzogranite and an aplitic dike (AP) at Punta Rossa MM; e) Porphyritic dike (PD) cutting the Metapelites and metasandstones (MPS) hornfels at Punta Rossa; f) Fe-Ax ± Qtz ± Adl + Ep (salband) vein in the Metapelites and metasandstones (MPS) at Punta Rossa.

are surrounded by a medium-grained groundmass. The latter is constituted by the same minerals with Bt and, sometimes, Tur (up to 7% and 3% respectively). Kfs generally prevail on Pl, but at Cale Gemelle area their proportions are inverted (see also Mittempergher, 1954). Accessory minerals include Ap, Zrn, Mag and Fe-Ox/Hydrox. Furthermore, monzogranitic xenoliths (made of Kfs and Pl) and metamorphic xenocrysts and aggregates (e.g., Grt) highlight the occurrence of interaction of this leucogranitic magma with the intruded rocks (see also Innocenti et al., 1997).

Minor bodies

Foliated porphyritic dikes

This type of dikes, never described before, was recognized in the Cale Gemelle area. They show a pervasive foliated texture made of Qtz, Ms and Bt with Qtz, Kfs, Pl porphyroclasts. Crystals of schorlitic Tur are also randomly present.

Pegmatitic veins

These veins (50% Qtz, 40% Ms, 10% Tur on average) are centimetric to decimetric in thickness, as described in previous studies (e.g., Roster, 1876; Millosevich, 1912; Palache et al., 1951). In the study area, these veins were found in the Punta Rossa outcrop, along Cala Corfù where they intrude the contact metamorphic rocks parallel to their main foliation.

Qtz veins

Several massive Qtz veins, generally 5-7 cm in thickness and not continuous in the field (up to 4 m in length), crosscut the granitoid in different areas. Qtz crystals are often euhedral and up to 5 cm long.

Ep and Ax(Fe) ± Qtz ± Adl ± Ep ± Act veins

Such often zoned hydrothermal veins are only visible within the hornfelses of Cala dei Ladri - Punta Rossa area (outcrops 3, 4, 5 and 6) and usually follow the main schistosity of the host rocks (Fig. 5f), but locally cross it at high-angle. Their thickness reaches 4-5 cm; the maximum length is around 5 m.

LITHOLOGY AND PETROGRAPHY OF THE CONTACT AUREOLE ROCKS

Lithostratigraphy

The scattered remnants of the contact metamorphic aureole outcrops are mostly exposed on the steep and isolated coast from Cale Gemelle - Cala dei Ladri to Cala Corfù through Punta Rossa in the southern part of the island (Figs. 2b and 6a). Another outcrop is present in the promontory south of Cala S. Maria along the western side of the isle (Fig. 2a).

In particular, six outcrops have been recognized (see Fig. 2a and b): Cala S. Maria (Outcrop 1, 1125 m^2), Punta Cale Gemelle (Outcrop 2, 15 m^2), Cala dei Ladri West (Outcrop 3, 6300 m^2), Cala dei Ladri East (Outcrop 4, 54000 m^2), Il Piano (Outcrop 5, 180000 m^2) and Punta Rossa (Outcrop 6, 1800 m^2). Their cumulative area covers about 2.3% of the total surface of the Montecristo Island. The maximum apparent thickness of the exposed successions of the aureole is 20-25 m in the widest Outcrop 5. All these metamorphic rocks are here grouped in a single stratigraphic-structural unit named Cala S. Maria-Cala dei Ladri Unit that structurally rests onto the Monzogranite (see later).

Three different lithologies were distinguished within the hornfels rocks according to their protoliths:.

Metagabbros

Massive light green metagabbros are present only within the Outcrop 1 (i.e., Cala S. Maria, Fig. 2a). It is often strongly fractured, especially in the southern part of the outcrop. The metagabbro is made up of green-grayish pyroxene crystals surrounded by white, more or less weathered whitish Pl. The size of pyroxene crystals is strongly variable, ranging from millimetric-centimetric (Fig. 6b) to 20 cm in the pegmatitic (or euphotid) gabbro (Fig. 6c) that is common in the northern part of the outcrop.

Metaserpentinites

They are described here for the first time and are present only in Outcrops 2 and 3 (i.e., Punta Cale Gemelle, Cala dei Ladri West, Fig. 2b). Such rocks are characterized by green to dark-green colours and often appear strongly foliated (Fig. 6 d and e) due to the orientation of the green Amp crystals. In Outcrop 3 these rocks are tectonically interposed between the Monzogranite and the overlying Metapelites and metasandstones (see Fig. 4). The latter contact is marked by a 30 cm-thick cataclastic horizon.

Metapelites and metasandstones

These lithotypes form three down-slope dipping bodies (Outcrops 3, 4 and 5) on the very steep coast of Cala dei Ladri area (Fig. 6a) and five smaller outcrops at Punta Rossa (Outcrop 6) (Fig. 2b).

According to Innocenti et al. (1997) and Rocchi et al. (2003a) the metasedimentary successions in the Outcrops 5 and 6 are calc-silicate hornfels derived from limestone, cherty limestone, chert and pelite alternations. Mittempergher (1954) described also chloritic calcschists. By contrast, our surveys reveal that most of the metasedimentary hornfelses are made up of alternating metapelites and metasandstones in all the preserved parts of the contact metamorphic aureole of Montecristo pluton, i.e., in Outcrops 3, 4, 5 and 6 (Cala dei Ladri west, Cala dei Ladri east, Il Piano and Punta Rossa). These hornfelses are well bedded and characterized by a millimetric to decimetric alternation of two distinct lithologies, light gray/yellowish phyllites and dark gray/black metasandstones (Fig. 6f). Moreover, the phyllites locally include brownish-red levels made of granoblastic to idiomorphic Grt (up to 1,5 cm in size) aggregates (Fig. 6g) that are locally common in the lowermost part of the successions (e.g., in the Outcrop 5). The Grt-bearing levels are usually 0.5-5 cm-thick, but locally they can exceptionally reach 50 cm or more (e.g., 1.2 m on the cliffs between Punta Rossa and Cala Corfù).

The contact with the underlying plutonic rock is generally marked by tectonic breccias. Locally [e.g., in the Outcrop 4) Cala dei Ladri and 6) Punta Rossa], intrusive contacts seem to be preserved (Fig. 6h) and marked by a thin tourmalinized horizon. Veins of Ep and/or Fe-Ax may be present in these metasedimentary rocks (Fig. 5f), particularly in the lower part of the Outcrop 6.

Petrography and mineralogy

Thirty two samples of the meta-ophiolitic and metasedimentary rocks of contact metamorphic aureole and fifteen samples of the magmatic and hydrothermal lithotypes were selected and examined through petrographic and X-ray diffraction (XRD) analyses (the data about the hornfels are summarized in Tables 1-2-3).

Metagabbros (Table 1)

They reveal a marked granoblastic/porphyroclastic texture, constituted by diopside, locally with augite (see also Mittempergher, 1954; Innocenti et al., 1997) and Pl megacrystals in a microcrystalline groundmass made up of Amp (Tr-Act), Pl (20-38 mol% An) and minor Tlc, Chl, pyroxene and Fe-Ox/Hydrox. Accessory minerals are Tur, Ep and Spn. Pyroxene porphyroclasts sometimes show a partial isorientation and frequent Amp blastesis along their rims. Pl is often broken and fractures are filled with Act ± Chl. Rare twinned Pl porphyroclasts show a zoning from 48-55% An in the core and 10% to 40% An to the rim. Isolated crystals and veins
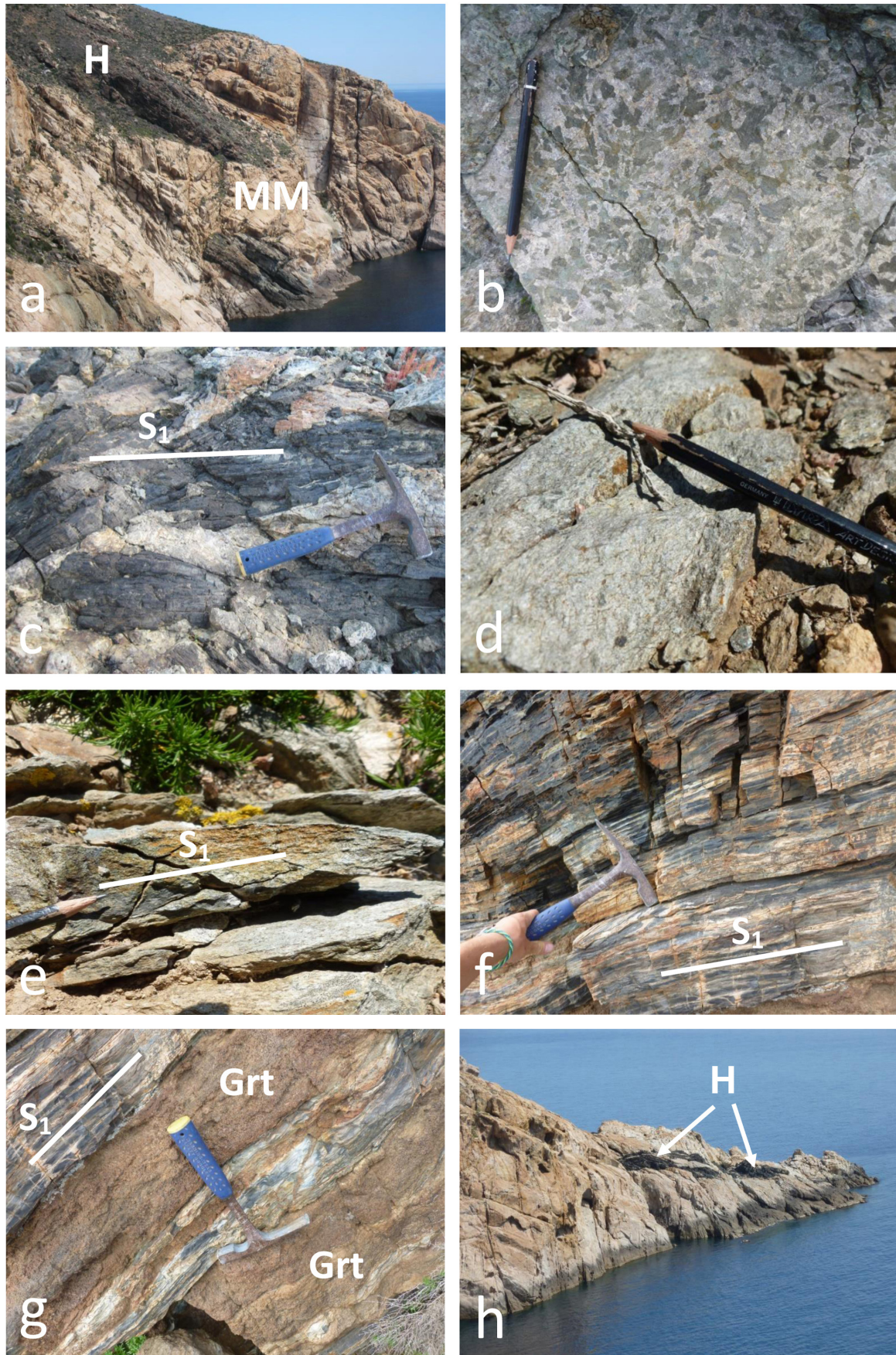
Fig. 6 - Pictures of the Cala S. Maria-Cala dei Ladri Unit hornfels rocks of the Montecristo pluton: a) Dark hornfels (H) above the Monzogranite (MM) at Cala dei Ladri; b) Isotropic Metagabbros at Cala S. Maria c) Foliated pegmatitic Metagabbro at Cala S. Maria; d) Metaserpentinites at Cale Gemelle; e) Foliated Metaserpentinites at Cala dei Ladri; f) Alternating phyllites and metasandstones in the Metapelites and metasandstones at Cala dei Ladri; g) Garnet-rich horizons (Grt) in the Metapelites and metasandstones at Il Piano; h) Scattered hornfels bodies (H) associated to the Monzogranite at Punta Rossa. S_1 = main foliation.

of sulfides and Fe-Ox/Hydrox are present, locally associated with pleochroic blue Tur (Srl-type) and green Ep.

In the southern part of the outcrop, the mineral assemblages and textures define at least three different types of metagabbros: the first one is characterized by a mylonitic texture made up of Pl and diopside porphyroclasts in a foliated groundmass made up of Pl, Qtz, Chl, Tr-Act and rare Bt and Spn (Fig. 7a); the second type exhibits a pervasive nematoblastic texture constituted by Act, and granoblastic bands or veins of Cpx, Qtz and Pl (50-55 mol% An); the third type is characterized by a coarse-grained granoblastic texture, with neo-formed diopside, sub-euhedral Pl (40-55 mol% An) and small Qtz lenses and veins. Ribbons and veins of Di and Pl (70-80 mol% An) were also recognized in places.

Metaserpentinites (Table 2)

They are mostly characterized by a porphyroclastic texture with pale-greenish Di and rare Opx. The fine- to medium-grained nematoblastic groundmass is largely dominated by Tr, with minor Cpx, Py and Fe-Ox/Hydrox (Fig. 7b and c). Green Ep, Aln, Zrn and Spn (with Rt inclusions), are the most common accessory minerals. The pyroxene porphyroclasts often show Tr isomorphic substitutions, pressure shadows and book shelf structures (Fig. 7d). Tr also fills the fractures in the Di porphyroclasts. In addition, the local presence of Hbl in Grt-bearing amphibolites is described in Mittempergher (1954). Ductile and brittle deformation zones with bands constituted by Qtz and Fe-Ox/Hydrox and light green Chl micro-veins, were also locally found.

Metapelites and metasandstones (Table 3)

Metapelites are by far the dominant lithotype of the metasedimentary outcrops. They exhibit a lepidoblastic to fine-grained, blasto-psammitic texture made up of Bt, fine-grained Qtz and minor Ms. The relative abundance of these components produced a typical alternation at the microscale with locally lenticular, more granoblastic/blastopsammitic layers of granular Qtz (0.5-2 mm) (Fig. 7e). Fe Ox/Hydrox bands are also locally present. In the Outcrops 4 and 5, Bt and Ms increase in size from the top to the bottom (i.e., toward the pluton) of the successions, where Tur-rich porphyritic veins and Grt-rich horizons are also commonly present.

The metasandstones are meta-quartzarenites and quartzitic-micaceous metasandstones that usually show a fine- to medium-grained granoblastic to blastopsammitic texture with abundant detrital Qtz and rare feldspars (e.g., Pl 15-38 mol% An) in a micaceous matrix made up of Bt, Qtz and minor Ms (Fig. 7f and g). At places, granoblastic metasandstones are characterized by Bt + Ms + Qtz ± Pl (30-45 mol% An) ± Cpx ± Spn. Local abundance of mica yields irregular, millimetric lepidoblastic alternations within the metasandstone beds. Concentrations of iron oxides/hydroxides locally form bands at the borders of the quarzitic layers.

HT minerals [Di-Hd + Pl 50-71 mol% An + Spn (often altered into Ilm) ± Grt, Qtz + Cpx] are present locally as patches (Fig. 7g) and veins crosscutting or parallel to the S_1 main metamorphic foliation (Fig. 7f, h and i). Fine-grained Wo can occur locally in the salband of the veins (see also Innocenti et al., 1997). Moreover, these veins often appear boudinated and folded together with S_1 (Fig. 7h and i). Finally, σ- and δ-type Cpx, Pl (47-58 mol% An) and Spn porphyroclasts (Fig. 7j) or their porphyroclastic aggregates are also recognizable.

The Ax veins, present in the Metapelites and metasandstones, particularly in the Punta Rossa area (Fig. 5f), are composed of green prismatic Ep (up to 1 cm) crystals (often as the salband) and light violet Fe-Ax (Mg/(Mg + Fe) = 0.19 - 0.21) and with inclusions of Sch (Innocenti et al., 1997) ± Act (Fig. 7k) ± Spn. Qtz, Adl, as well as Py and Ccp, can be present in the inner part of the veins (Fig. 5f).

Recrystallizations and pervasive foliations characterize most of the Metapelites and metasandstones outcrops, but locally in the Outcrop 6 and in the upper part of the Outcrops 4 and 5 successions, the metamorphism is of a very low-grade. In fact, there the metasandstones exhibit the original clastic sedimentary structure made of angular mono- and polycrystalline Qtz in a slightly recrystallized pelitic matrix made up of Bt, Ms, Fe-Ox/Hydrox and Qtz. The degree of recrystallization and the content in Ms blasts (up to 25 %) clearly increases toward the base of the metasedimentary successions over a vertical distance of 10-15 meters (e.g., in Outcrop 5).

Grt-rich skarn bands, which are almost entirely constituted by granoblastic Grs-Adr (Fig. 7l), are common in the lowermost parts of the successions (e.g., in the Outcrop 5). Here, the metapelitic host rocks (see Fig. 6g) are made up of Bt + Ms + Qtz ± Pl (47-60 mol% An) ± Cpx ± Spn, whereas the skarn bands are constituted by associations of Grt (Grs_{59-67}, Adr_{38-29}, Alm_{3-4} in Innocenti et al., 1997) ± Cpx ±Ep ± Tr ± Qtz ± Bt ± Pl (56-68 mol% An) ± Fe-Ox/Hydrox.

STRUCTURAL DATA

The main tectonic structure of the Monzogranite is the Cala Maestra-Cala Corfù Fracture Zone (MCFZ in Innocenti et al., 1997), a NW-SE oriented shear zone with a length of about 3 km and a width of 0.5 km , exposed along the southwestern portion of Montecristo Island (Fig. 2). The major brittle and ductile structures in the Monzogranite are present within the Cala Maestra-Cala Corfù Fracture Zone. Other minor sheared areas are located immediately south of it, i.e., in the eastern side of Cale Gemelle and at Punta Rossa.

In order to reconstruct the processes connected to the emplacement and exhumation of the pluton, structural data were collected in the Cala S. Maria and Cala dei Ladri - Punta Rossa areas where both the magmatic/hydrothermal bodies and the hornfels are well exposed. Ductile and brittle structures defined in the two main units will be described according to their relative chronology (see Fig. 4 and Table 4).

Magmatic/hydrothermal rocks

The structural data allow to define several successive deformation events named as M-magmatic in Table 4:

Ductile structures

Magmatic foliation (M_1mf event in Table 4)

Primary foliation defined by the alignment of Kfs phenocrysts in the Monzogranite is related to the magmatic flow (Fig. 3d, LPO = Lattice Preferred Orientation in Table 4). This structure shows a E-W to NNW-SSE and NW-SE to NNW-SSE strikes in the southern and in the western part of the island, respectively.

Mylonites (M_1my event in Table 4)

Mylonitic shear bands (see also Innocenti et al., 1997) deform the Monzogranite and are particularly well exposed in the Cale Gemelle area and northwest of Punta Rossa (Figs. 2b, 8a and b). Here, these locally mylonitic bands have a thickness ranging between 10 cm and 2 m. Locally, the mylonitic foliation flattens the original holocrystalline texture
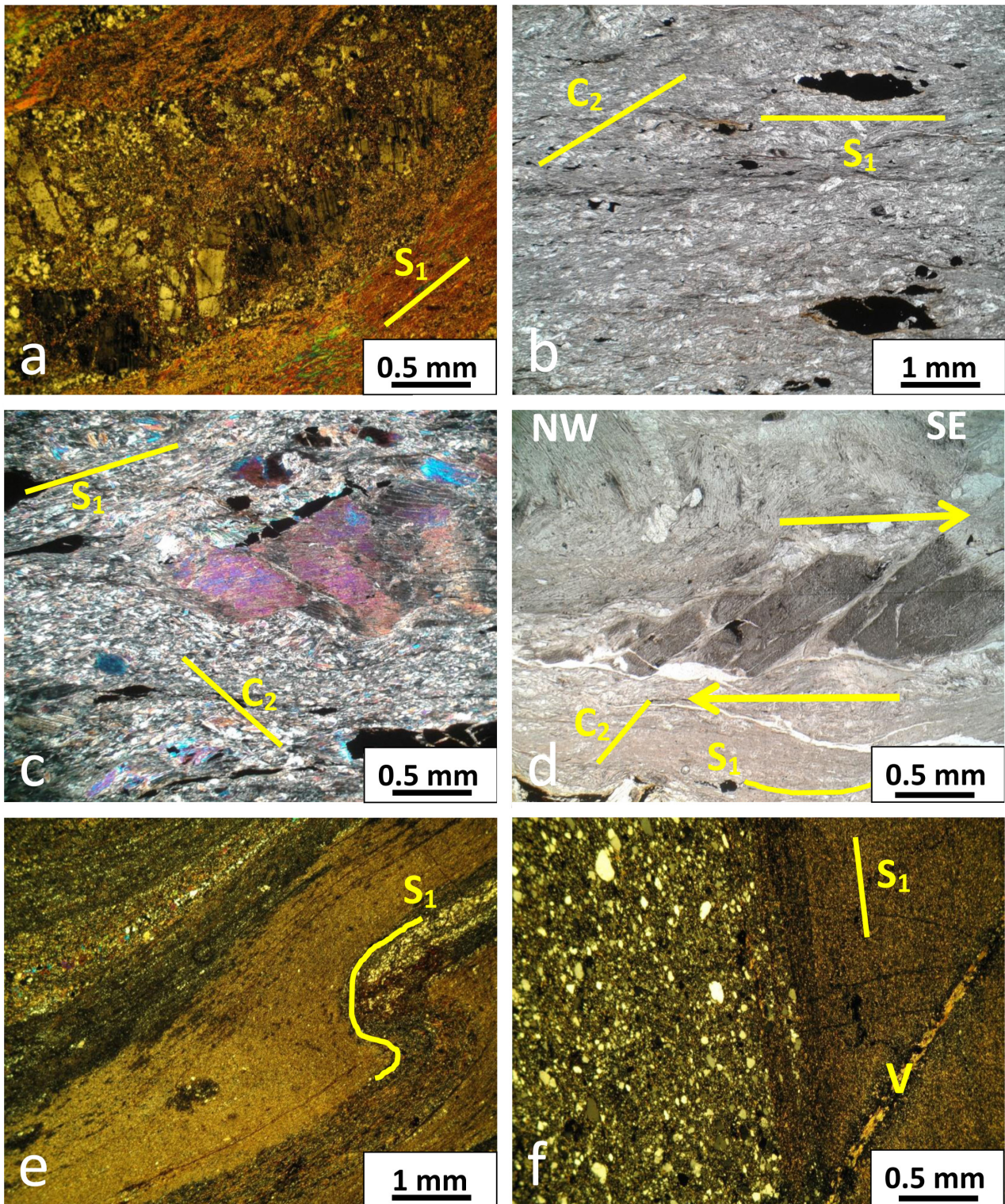
Fig. 7 - Photomicrographs of the hornfels of the Montecristo pluton: a) Mylonitic metagabbro in the Outcrop 1. Cross-polarized light; b) S_1 foliation deformed by zonal C_2 cleavages in the Metaserpentinites in the Outcrop 3. Plane-polarized light; c) Amphibolitized Cpx porphyroclast in the foliated tremolite groundmass of the Metaserpentinites in the Outcrop 2. Cross-polarized light; d) Book-shelf structures in the Metaserpentinites in the Outcrop 2. Sinistral antithetic microfaults in the stepped fragmented amphibolitized porphyroclast defining a dextral sense of shear synkinematic to S_1 (cfr. Passchier and Trouw, 1996). Plane-polarized light; e) Minor tight-close F2 fold deforming lithological millimetric alternations// S_1 in the Metapelites and metasandstones at Il Piano. Cross-polarized light; f) Quartzic metasandstone passing to a metapelitic intercalation in the Metapelites and metasandstones . V = vein with HT minerals (Cpx + Pla/Pll) of the Cala dei Ladri area. Cross-polarized light; g) Quartzitic metasandstone with recrystallized matrix and Cpx and Tur plagues in the Metapelites and metasandstones of the Cala dei Ladri area. Cross-polarized light; h) Tight F2 fold with C_2 crenulations that deforms S_1 and //Cpx-rich veins in the Metapelites and metasandstones of the Cala dei Ladri area. Cross-polarized light; i) Close F2 fold, that deforms S_1 and //Cpx-rich veins, with associated discrete-type crenulation cleavage (S_2) in metapelites of the Metapelites and metasandstones in the Cala dei Ladri area. Cross-polarized light.; j) σ-type mantled Cpx porhyroclast, pointing to a dextral sense of shear syn-kinematic to S_1 (cfr. Passchier and Trouw, 1996), within the metapelites of the Metapelites and metasandstones in the Cala dei Ladri area. Cross-polarized light. k) Fe-Ax (Ax, white areas) and Act fibers with Ep salband in the Metapelites and metasandstones of the Punta Rossa area. Cross-polarized light; l) Idiomorphic Grt and intercrystalline Tr in a Grt-rich skarn level in the Metapelites and metasandstones of the Outcrop 5. Cross-polarized light.
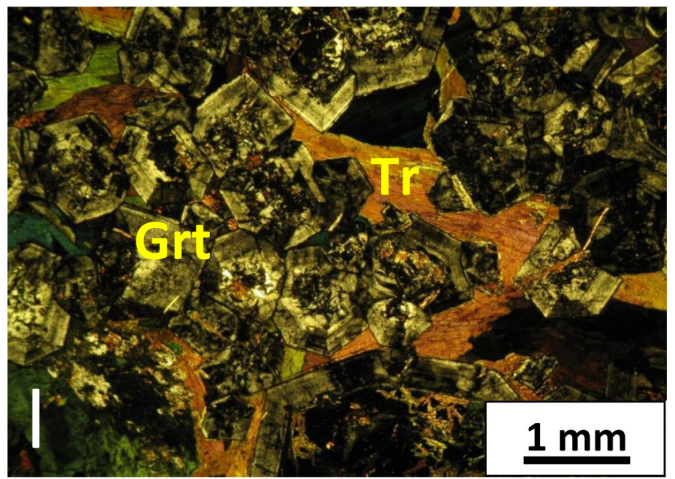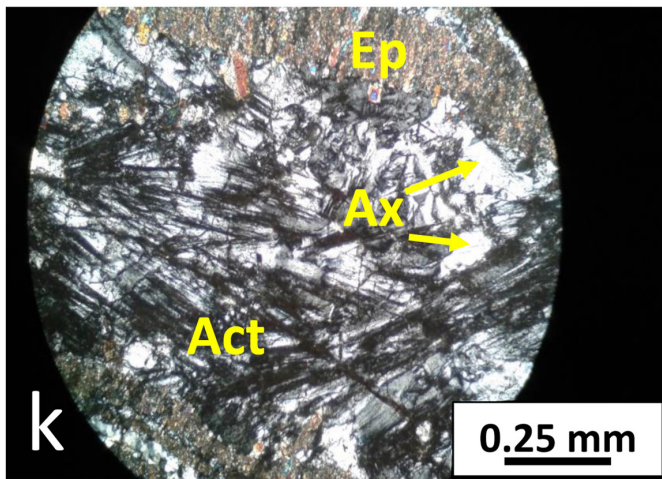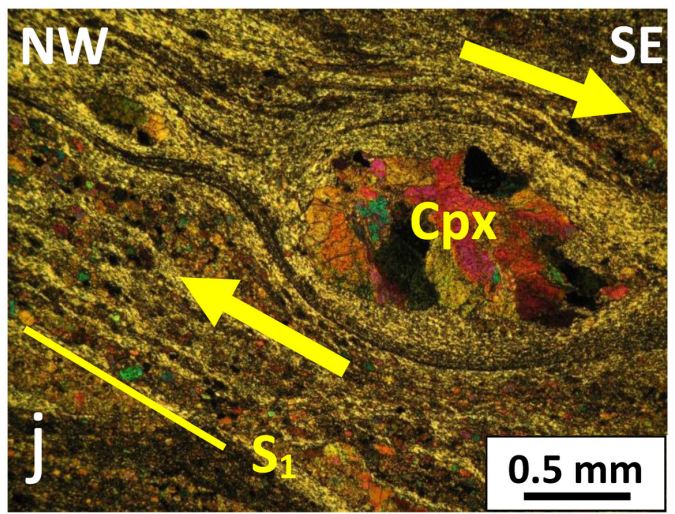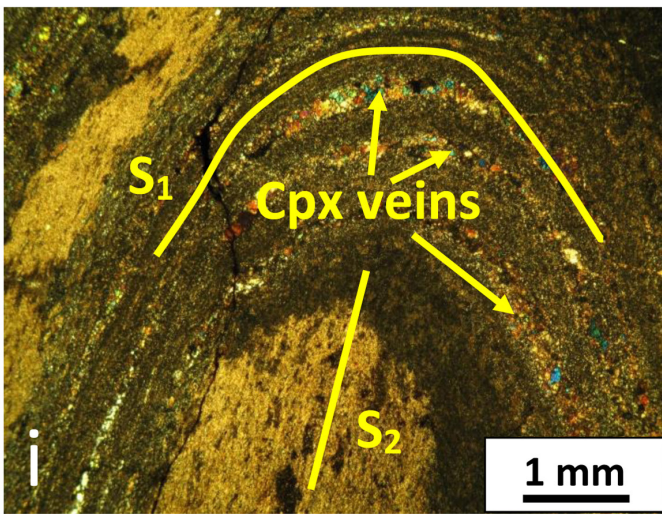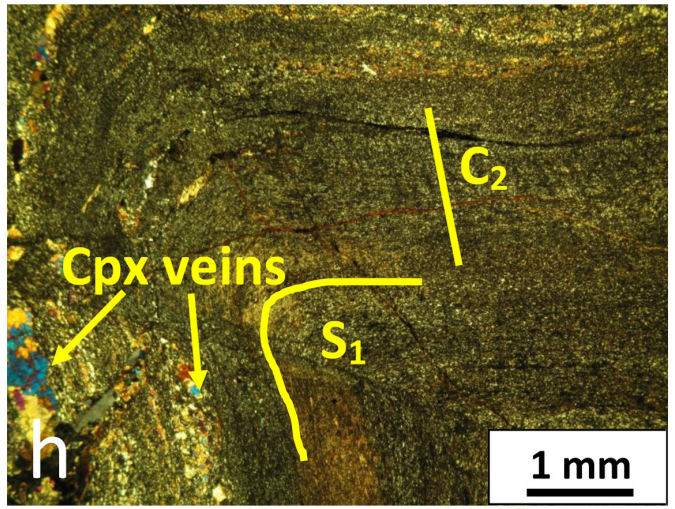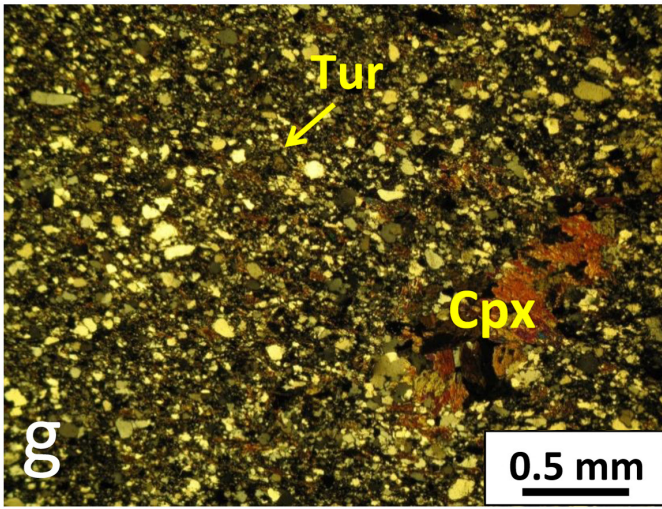
Fig. 7 (*continues*)

Table 4 - Deformation evolution of the magmatic bodies and the Cala S. Maria-Cala dei Ladri Unit hornfels from the Montecristo Island.

EVENT	TYPE of event and RHEOLOGY of country rocks	ORIENTATION (strike)	STRUCTURES	SHEAR	NOTES
M1mf	PRIMARY Ductile in MM	E-W to NNW-SSE (southern areas), NW-SE to NNW-SSE (western area)	LPO Mkx	-	Monzogranite (7.1 Ma)
M1my	Secondary Ductile in MM	NW-SE (Cale Gemelle area)	Mylonites	sinistral shear Top to the NW	
D1	SECONDARY Ductile	NE-SW to ENE-SSW (Outcrops 3, 4, 5, 6)	S1, meso- and boudinage of garnet layers, sigmoids, bookshelf meso- and micro-structures, mylonites in MG	Top to the SE	Synkinematic/thermometamorphic assemblage and layering (Presumably influenced by local stress and radial to the uplift center)
D2	SECONDARY Ductile	NE-SW to ENE-SSW (C2 and S2, Outcrops 3, 4, 5) NE-SW (axes of folds in Outcrops 3, 4, 5, 6, shear plane in Outcrop 2)	C2 crenulation cleavage, F2, S2	Top to the SE	Folds vergence to SE (Presumably influenced by local stress and radial to the uplift center)
M2	SECONDARY Brittle	NW-SE to NNW-SSE (main) or NNE-SSW to NE-SW	Aplitic dikes (AP)	-	Magmatic event
M3	SECONDARY Brittle	about N-S to NNE-SSW	Qtz+Tur veins (QT)	-	Hydrothermal event
D3	SECONDARY Brittle	40° WNW-dipping (Outcrop 1); horizontal to 50° SE-dipping (Outcrop 2, 3, 4, 5, 6)	Cataclasitic horizons and tectonic contacts		Creation and emplacement of the roof pendant plates
M4-D4	SECONDARY Brittle	NW-SE (main) and NE-SW	High-angle Joints	-	Extensional, mostly unfilled jointing (prosecution of the unroofing and cooling of the pluton)
M5-D5	SECONDARY Brittle	NNW-SSE (TPnb) and NE-SW to ENE-WSW (TPb)	Tourmaline-bearing porphyritic dikes (TPD)	-	Magmatic event
M6-D6	SECONDARY Brittle	WNW-ESE and subordinately ENE-WSW	Porphyritic dikes (PD)	-	Magmatic event
M7-D7 (MCFZ)	SECONDARY Brittle and transitional ductile- brittle	Generally with WNW-ESE strike, ENE-WSW (dextral), WNW-ESE to NW-SE and NNW –SSE (sinistral)	High angle normal, transcurrent or transtensive micro- and mesofaults, protomylonites and pseudotachylites, S-C structures, φ and σ microstructures, en-echelon veins	Overall sinistral Riedel system along the MCFZ	Protomylonitic shear zones, and pseudotachylites (presumably influenced by regional stress)

Events: M in the magmatic rocks (M1mf = magmatic flow, M1my = mylonitic event), D in the hornfels.
LPO Mkx= Lattice Preferred Orientation of Kfs megacrysts.

and causes the fragmentation of the Kfs phenocrysts, that frequently display "book shelf" or even "boudinage" structures. At the microscale, the mylonitic texture is made up of strained Qtz and Kfs phenocrysts and of granitoid clasts in a grano-lepidoblastic foliated matrix with Bt and heterodimensional granular Qtz, Kfs, Pl and Tur. Kinematic indicators at the meso- and microscale are mainly S-C structures, σ-type rotated and fragmented porphyroclasts, and elongated refer-ence bodies like mafic enclaves. The mineralogical lineations and, particularly, the kinematic indicators present on the XZ plane (e.g., S-C planes, mantled porphyroclasts, stepped faults) allow to define the sense of shear according to Passchier and Trouw (1996), Davis and Reynolds (1996), Fossen (2010) and Mukherjee (2014). In the Cale Gemelle outcrops, S-C mesostructures are related to a NW-SE-oriented sinistral shear (Fig. 8a and b).
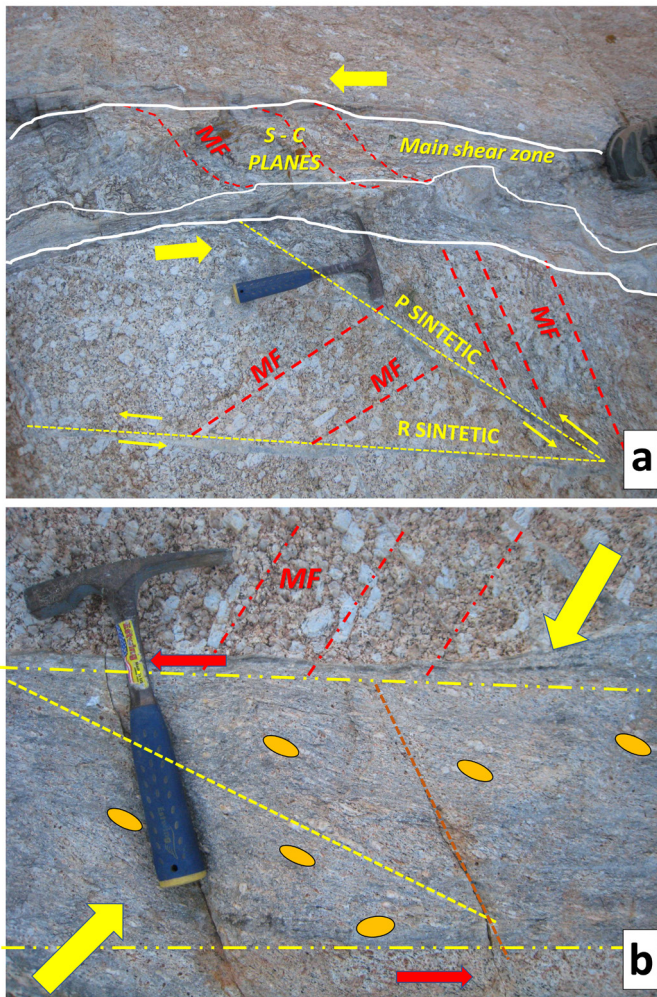
Fig. 8 - a) Mylonitic horizon in the Monzogranite at Cale Gemelle; b) magnification of the shear zone. In a): on XZ plane, S-C planes define a sinistral sense of shear for the main shear zone related to a Riedel syntetic shear (P and R); in b): on XZ plane, mylonitic foliation with elliptical objects. Note that the X axe is parallel to mylonitic foliation and define a pure shear synkinematic to a simple shear that is typical of a transpressive regime. MF = Magmatic Flow.

Brittle structures

Several superimposed systems of joints and faults affected the Monzogranite in different times. Most of them were filled by dikes and hydrothermal veins. Therefore, their overprinting relations are used for a relative chronology of the fracture networks systems from the oldest to the youngest (see Fig. 9):

System of Aplitic dikes (M$_2$ event)

In the whole island the dip of Aplitic dikes is generally sub-vertical with a main NW-SE to NNW-SSE or NNE-SSW to NE-SW strike. The NNW-SSE (mean 330°-150°) strike is more common in the study area (Fig. 9a).

System of Qtz and Tur veins (M$_3$ event)

The strike of the Qtz and Tur veins is from about N-S to NNE-SSW and displays a sub-vertical or steeply westward dip direction (Fig. 9b). Locally they displaced the Aplitic dikes with centimetric-decimetric throws (Fig. 10a).

System of high-angle jointing (M$_4$ event)

High-angle, pervasive and sub-parallel, mostly unfilled joints and minor transcurrent faults with centimetric throw (Fig. 10b), revealed by differential erosion, are the most diffused brittle elements in the Monzogranite and crosscut also the Aplitic dikes and the Qtz and Tur veins. Joints show a main NW-SE orientation, but NE-SW directions are also observable (Fig. 9c), even if less continuous in the field. Locally these joints are filled with hydrothermal minerals (mostly quartz). In the Punta Rossa area, these structures are crosscut by the Tur-bearing porphyritic dikes and veins and the Porphyritic dikes (Fig. 10c).

System of Tur-bearing porphyritic dikes and veins (M$_5$ event)

Two different orientations can be defined for the two types of sub-vertical Tur-bearing porphyritic dikes and veins (Fig. 9d and e): the lighter TPDnb are characterized by NNW-SSE (mean 350°-170°) strikes, whereas the following darker TPDb show a NE-SW to ENE-WSW (mean 50°-230°) strike.

System of Porphyritic dikes (M$_6$ event)

The Porphyritic dikes have a sub-vertical or a steep dip toward NNE-NE with WNW-ESE and subordinately ENE-WSW strikes (Fig. 9f). Qtz-filled orthogonal joints frequently cross the Porphyritic dikes.

System of later normal faults and jointing (M$_7$ event)

High angle normal faults, often characterized by cataclasites, striated planes and jointing can be recognized frequently in the Monzogranite (Fig. 10d, e and f), as well as transtensive faults (with a 20° pitch). They are significantly more common along the Cala Maestra-Cala Corfù Fracture Zone (see locations in Fig. 2b, e.g., at Punta Rossa) and locally cross-cut the high-angle joints, the Tur-bearing porphyritic dikes and veins and the Porphyritic dikes in the Monzogranite. Other brittle structures (tension gashes in Fig. 10g) and transitional brittle-ductile structures related to this event (protomylonites, according to Trouw et al., 2009, in Fig. 10h and pseudotachylites in Fig. 10i and j) are recognizable in the Monzogranite in the Punta Rossa, Cala Corfù and Cale Gemelle areas. The protomylonites (Fig. 10h) show a mortar texture with many heterodimensional Monzogranite porphyroclasts in a reduced finer-grained, Qtz- and Pl-rich, granular matrix that is characterized by a rough foliation. The black pseudotachylites within the Monzogranite are centimetric in thickness (generally 2-4 cm, max 10 cm) and some meters in width (generally less than 10 m) (Fig. 10 i and j). They consists of an highly brecciated Monzogranite with a matrix made up of black Tur (Srl), Fe Ox/Hydrox and a low amount of glass (between 4 and 8% wt).

The strike of the high angle, locally transtensive faults and joints is mainly WNW-ESE (Fig. 9g), whereas the orientation of the protomylonites is from WNW-ESE to NW-SE and ENE-WSW (Fig. 9 h) and mainly NW-SE for the pseudotachylites (Fig. 9i). The sense of movement of these shear structures (see Fig. 2) was locally defined by kinematic indicators (as lunate tectoglyphes, slikenside flutes, R and T fractures). In particular, the sense of shear of the transtensive faults is ENE-WSW dextral in the Punta Rossa outcrop, WNW-ESE sinistral at Cala Corfù and NNW-SSE sinistral sense at Cala S. Maria and Cala Maestra. In the western side of Cala Corfù, Tur-rich en-echelon joints indicate a sinistral sense of movement (Fig. 10g). The pseudotachylites show a sinistral sense in the Cala S. Maria - Cala Maestra area (Fig. 10j) and dextral at Punta Rossa; the sense of shear of the protomylonite in the western part of the Cala dei Ladri is sinistral.

Hornfels

Metagabbros

They lie onto the Monzogranite in Outcrop 1 through an evident tectonic contact (Fig. 4) characterized by a 290/40 dip direction that is frequently highlighted by cataclasites and fault gouges. The intense fracturing and the abundant vegetation make the meso-structural analysis of these rocks difficult. Anyway, a metamorphic foliation S_1 [S_1 = Tr + Pl (10-40 mol% An) ± Qtz ± Bt + Spn] and mylonitic horizons (Fig. 7a), highlighted by the overall Amp isorientation, can be locally recognized at the mesoscale showing the same attitude as the basal tectonic contact, that dips toward west.

Metaserpentinites

The contact of this unit with the pluton is tectonic too (Fig. 4) and in both Outcrops 2 and 3 it is marked by a cataclastic 10-15 cm-thick horizon dipping toward SE. The main schistosity plane S_1 (S_1 = Tr ± Fe Ox/Hydrox, Fig. 7b) dips at high to middle angle toward SE/SSE (140/75 and 160/50 in the Outcrops 2 and 3, respectively). δ- and σ-type mantled and "*book shelf*" structures often characterize the amphibole porphyroclasts (after pyroxenes) within S_1 (Fig. 7c and d) and point to a top to SE sense of shear.

C_2 zonal crenulations are also present (Fig. 7b, c and d). Even if the S_1 schistosity of the amphibolites can locally appear parallel to the hornfels-granitoid boundary, a general sharp angular structural unconformity separates the monzogranitic surface (dipping about 20° toward SE) and the metamorphic foliation. In Outcrop 3, the Metaserpentinites lie geometrically below the the Metapelites and metasandstones through a highly-weathered, 30 cm thick cataclastic layer, whose orientation roughly coincides with the main metamorphic schistosity plane.
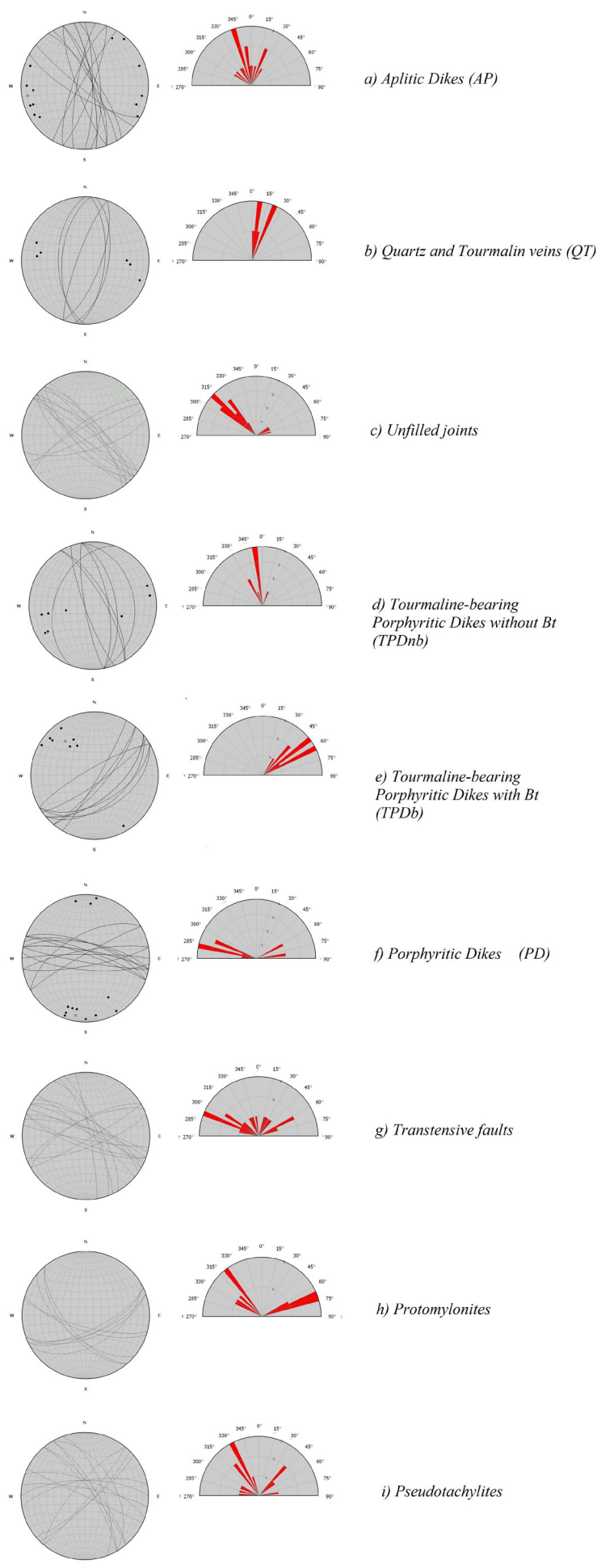
Metapelites and metasandstones

Compared to the previous formations of the Cala S. Maria-Cala dei Ladri Unit, the Metapelites and metasandstones exhibit a large variety of ductile and following brittle structures related to different events (D) that are described below from the oldest (see Fig. 12 and Table 4):

Ductile structures

D_1 is represented by a mm/sub-mm- thick, main continuous foliation S_1 = Bt + Qtz ± Pl (15-38 mol% An) ± Ms or Bt + Ms + Qtz ± Pl (30-45 mol% An) ± Cpx ± Spn that is subparallel to the lithological boundaries (Figs. 6f and 7 f) and with a NE-SW to ENE-SSW strike in Outcrops 3, 4, 5 and 6. S_1 is characterized by a strong Bt isorientation. *Boudinage* is locally common (Fig. 11a) and particularly evident in the Grt-rich layers, producing 5 cm to 20 cm-long boudins (Fig. 11b). *Book-shelf* structures and rotations of porphyroclasts (Fig. 7j) as well sigmoidal structures (Fig. 11c) occur in places and indicate a top to the SE sense of shear. S_1 is usually oriented sub-parallel to the roof surface of the granitoid body; S_1 dip variations are present locally due to D_2 folding. In particular, dip direction of S_1 planes is to the SSE-SE (160°/40° on the average), whereas dip angles are extremely variable, from high values (50° in Outcrop 3 and 4 or even up to 90° in Outcrop 6) to almost flat attitudes (10° in Outcrop 5) (Fig. 12).

Fig. 9 - Poles and cyclographic plots (Schmidt, lower hemisphere) and rose diagrams of the strike of the superimposed dikes/hydrothermal veins and brittle structures in the magmatic rocks according to their relative timing (from the oldest at the top downward).

a) Aplitic Dikes (AP)

b) Quartz and Tourmalin veins (QT)

c) Unfilled joints

d) Tourmaline-bearing Porphyritic Dikes without Bt (TPDnb)

e) Tourmaline-bearing Porphyritic Dikes with Bt (TPDb)

f) Porphyritic Dikes   (PD)

g) Transtensive faults
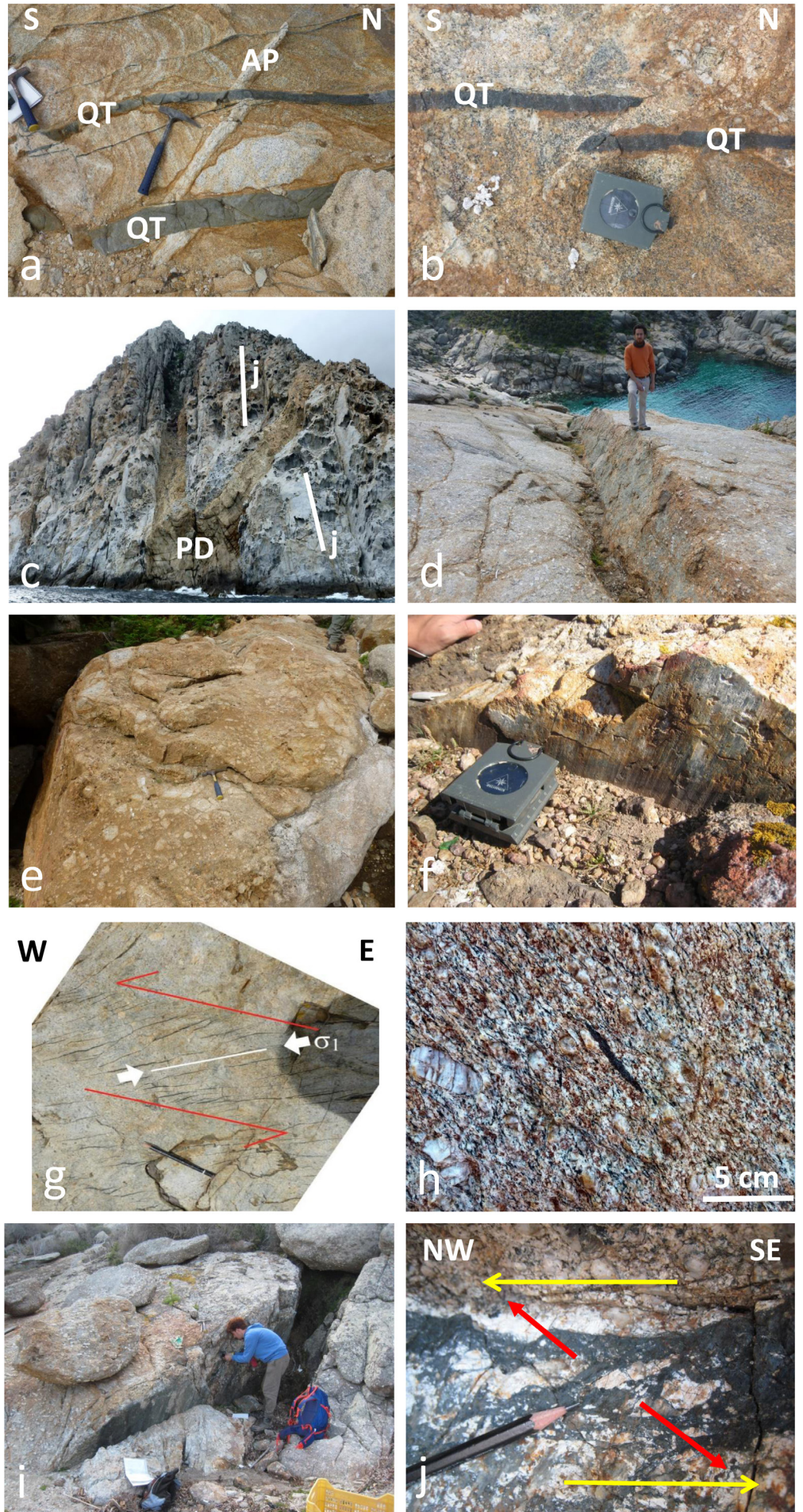

h) Protomylonites

i) Pseudotachylites

Fig. 10 - Brittle structures in the magmatic rocks: a) Millimetric- to centimetric black Qtz and Tur veins (QT) filling minor sinistral transcurrent faults that displace a whitish Aplitic (AP) in the Monzogranite at Punta Rossa; b) Minor dextral transcurrent faults displacing black Qtz and Tur veins (QT) at Punta Rossa; c) Porphyritic dikes (PD) infilling and crossing the sub-vertical D_4 joint system (j) at Punta Rossa area; d) Later high-angle faulting in the Monzogranite at Cala Mendolina; e) Cataclasite of a later high angle fault in the Monzogranite at Cala Corfù; f) Striated structures in a later normal fault at Cala Maestra. Downdip lineation on XY plane; the presence of grooves allows to define a vertical normal fault; g) En-echelon joints and stepped microfaults consistent with a sinistral sense of shear and a E-W directed σ1 at Cala Corfù; h) Protomylonite in the Monzogranite in the Cala dei Ladri area; i) Decimetre-thick black pseudotachylite horizon in the Monzogranite at Cala S. Maria; j) Top-to-the-NW shear indicators in a pseudotachylite at Cala S. Maria.
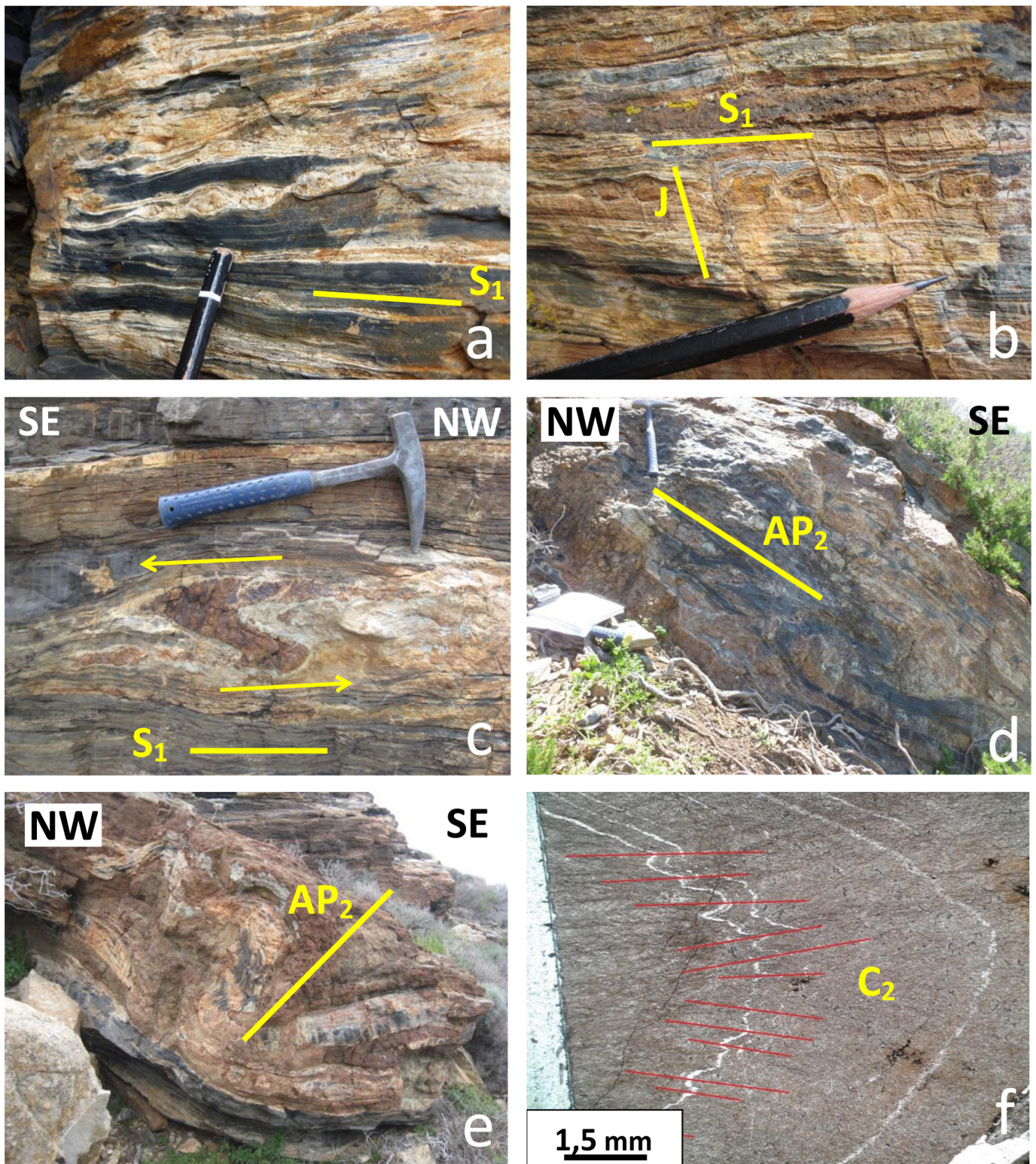
Fig. 11 - Ductile and brittle structures in the Metapelites and metasandstones hornfels: a) Boudinage // S_1 of quartz-rich layers at Il Piano; b) Boudinage of a garnet-rich layer //S_1 and following high-angle jointing (J) at Il Piano; c) Sin-D_1 sigmoid structure of a garnet-rich layer (at Il Piano) pointing a top-to-the-SE sense of shear; d) Recumbent-type F_2 isoclinal folds at Cala dei Ladri; AP_2=Axial plane of F2; e) Overturned/asymmetric - type F2 folds at Il Piano; AP_2=Axial plane of F2; f) Photomicrograph of a close-type F_2 with zonal crenulation cleavage (C_2). Plane-polarized light; g) Photomicrograph of a tight/isoclinal-type F2 with zonal crenulation cleavage (C_2) and later jointing. Plane-polarized light; h) Z-type D_2 drag folds at Il Piano, AP_2=Axial plane of F2; i) M- and S-type D_2 drag folds deforming a garnet-rich layer at Il Piano; j) F2 chevron-type similar fold at Punta Rossa. AP_2=Axial plane of F2; k) Centimetric-spaced unfilled jointing (j) affecting Metapelites and metasandstones at Il Piano; l) Dextral transcurrent fault intersects Metapelites and metasandstones (MPS) and some Tur-bearing porphyritic dikes (TPDnb, view from W) at Punta Rossa.
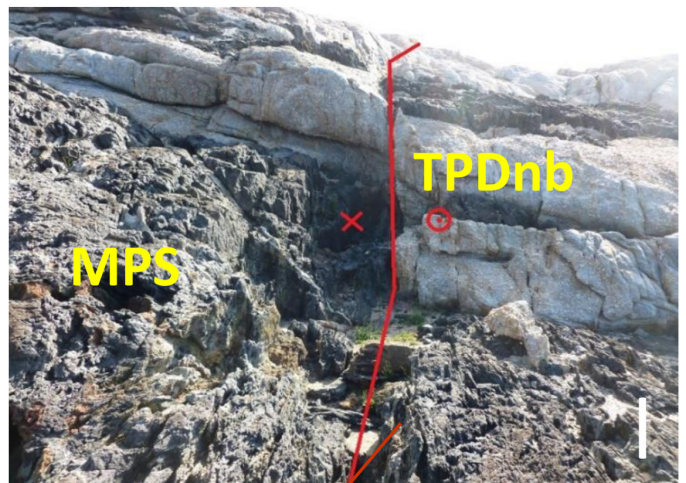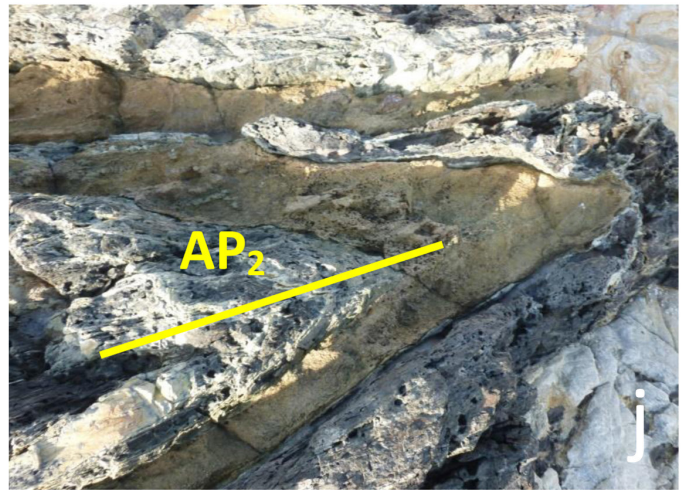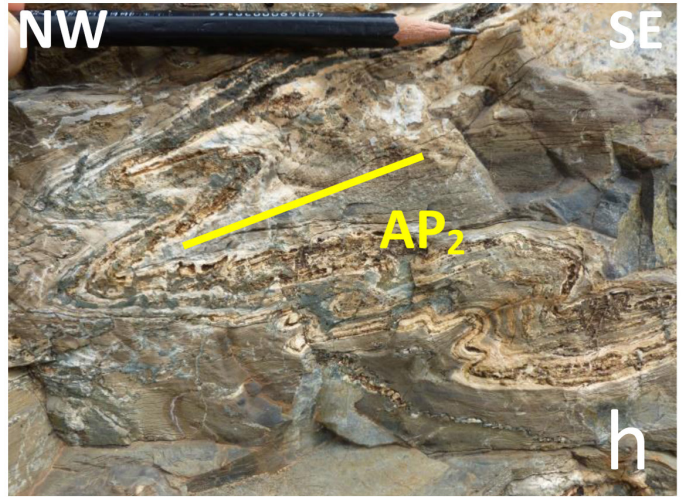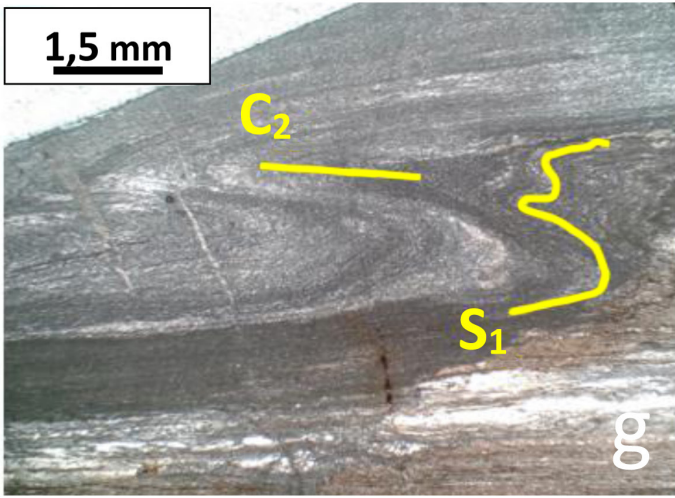
Fig. 11 (*continues*)

D_2 is related to the folding of S_1 that is recognized at the meso-scale in all the outcrops. In particular, D_2 is characterized by open/close to nearly isoclinal metric folds of type 1B, 1C and 2 of Ramsay (1967) class (Figs. 7h and i, 11d and e). The attitude of their axial planes mostly shows dips at middle-high angle toward SE (160/50 dip direction average value) (Fig. 12). These folds are often recumbent (Fig. 11d), but, locally, are overturned with axial planes plunging to NW (Fig. 11e) and their axes are parallel to the boundaries of the pluton. The axial plane foliation forms a millimetric to centimetric spaced, generally zonal, crenulation cleavage (C_2 in Fig. 11f and g), with strike similar to that of S_1. D_2 centimetric- to decimetric-sized drag folds, deforming limbs and hinges of main D_2 folds can be frequently recognized (Fig. 11h and i). In Outcrop 6, SE-verging chevron-type fold are also present (Fig. 11j). Cpx-bearing veins within S_1 are locally deformed by F_2 folds and by their foliations (Fig. 7h and i). Finally, the downward increase of the ductile behavior of the hornfels during D_2 folding is testified by discrete-type crenulation cleavages ($S_2 = Bt \pm Ms \pm$ Fe Ox/Hydrox) that characterize tight to isoclinal F_2 folds in the lower part of some outcrops (e.g., in Outcrops 4, 5 and 6), producing a composite schistosity ($S_2//S_1$) along the limbs (Fig. 7i).

Brittle structures

D_3 is referred to the tectonic contacts, often underlined by cataclastic horizons at the base of the Cala S.Maria-Cala dei Ladri Unit and inside of the already folded hornfels succession (e.g., between the Metaserpentinites and the Metapelites and metasandstones in Outcrop 3). Their attitude is 40° WNW-dipping in Outcrop 1 and horizontal to 50° SE-dipping in the southern outcrops (Outcrop 2, 3, 4, 5).

D_4 produced the more common brittle deformation structures in the hornfels that are represented by unfilled joints (Fig. 11k) and minor normal faults at the meso- and microscale, particularly in the widest Outcrops 5 and 6. Two sets of brittle structures can be identified in both Outcrops 5 and 6: an overall main NW-SE and a secondary NE-SW system that intersect S_1 at high angle (Fig. 12). The patterns of the two main sets of joints in the hornfels are very similar to those described for the high-angle unfilled joint systems defined in the magmatic bodies below the basal cataclastic horizons of the hornfels plates (cfr. Fig. 9c), likely suggesting their correlation. The joints in the hornfels are crosscut and locally intruded by the Tur-bearing porphyritic dikes and veins and the Porphyritic dikes (Fig. 10c).

D_5 is referred to the fractures intruded by the Tur-bearing porphyritic dikes and veins, i.e., TPnb and TPb that show NNW-SSE and NE-SW to ENE-WSW strikes respectivelly

D_6 is related with main WNW-ESE fractures that are intruded by the Porphyritic dikes at places.

D_7 is characterized by high angle normal, transcurrent or transtensive (Figs. 11l and 12), generally WNW-ESE to NW-SE-striking faults, that cut both the Monzogranite and the overlying hornfelses, particularly in the Punta Rossa area (Outcrop 6). They are locally characterized by decimetric to metric throws, displacing the Metapelites and metasandstones, the Tur-bearing porphyritic dikes and veins and the Porphyritic dikes (Figs. 2b and 11l), and are frequently emphasized by centimetric cataclastic bands and locally by tectoglyphes (e.g., slickensides) on the fault plane.

DISCUSSION

Stratigraphy

The 1:5000 scale geological survey points to a more complex lithostratigraphic architecture of the hornfels of the Montecristo Island (here grouped into the Cala S. Maria-Cala dei Ladri Unit) compared to that reported by Innocenti et al. (1997). In fact, new lithologies have been found (e.g., Metaserpentinites) and we defined the alternating metapelites and metasandstones (Metapelites and metasandstones) as the dominant hornfels rocks in all the outcrops of the metasedimentary successions. Conversely, a very limited amount of calcsilicate hornfels are present, i.e., in the lower parts of the Cala dei Ladri outcrops. In any case, we agree with Innocenti et al. (1997) and Rocchi et al. (2003a): all the successions of the Montecristo hornfels pertain to the oceanic Ligurian realm. Moreover, our data suggest the direct correlation of the Montecristo contact metamorphic aureole with that of the Mt. Capanne in western Elba Island (see Pandeli et al., 2018). The lack of HP-LT mineral associations in the Montecristo Island metamorphic rocks cannot completely discard their attribution to the Ligurian-Piedmontese successions (i.e., the typical "Schistes Lustrés" of NE Corsica, in the islands of Gorgona and Giglio, and Argentario Promontory: Jolivet et al., 1998; Orti et al., 2002; Elter and Pandeli, 2002) since the HT metamorphism might have strongly overprinted their early tectono-metamorphic evolution. Anyway, the survival of HP-LT mineral associations in hornfels rocks is testified in the Ligurian-Piedmontese Acquadolce Unit, of eastern Elba Island in spite of medium/high-grade contact metamorphism (Pandeli et al., 2001; Bianco et al., 2015). So, more appropriately, we propose that the protoliths of the Metagabbros, Metaserpentinites and Metapelites and metasandstones likely belong to the Ligurian successions and, in particular, to those of the Internal Ligurian Units (see Marroni and Pandolfi, 1996; Marroni et al., 2004; Nirta et al., 2005; Principi et al., 2015). Most of the metasedimentary rocks of Montecristo metamorphic aureole consist of metapelite with quartzitic metasandstone intercalations. This peculiar alternance is well-known in the Ophiolite Unit (or Vara Unit) of the Internal Ligurian Units in Southern Tuscany. In particular, a Quartzarenitic Member, associated to the Early Cretaceous Palombini Shales, was defined in the Colline Metallifere by Lazzarotto (1967) and in the Mt. Amiata area by Pandeli et al. (2005); moreover, the presence of Grt-rich skarn levels within the Metapelites and metasandstones likely suggests the presence of original calcareous-marly intercalations. In this frame, the protolith of these successions could be attributed alternatively to parts of the Early-Late Cretaceous Lavagna Shales (M. Verzi Slates in Boni et al., 1969) from the Vara Unit in eastern Liguria, constituted by shales alternated with sandstones, calcarenites and marls. Similar considerations were proposed by Spohn (1981) and Pandeli et al. (2018) for the pelitic-arenaceous succession at the top of the of the Punta Nera - Punta Polveraia Unit hornfels of the Mt. Capanne pluton in the Marciana area. Instead, at least part of the metapelites with Grt-rich horizons and rare calcschists intercalations in the Cala dei Ladri area may be correlated to the Palombini Shales.

The Outcrop 3 deserves a more detailed discussion because of the tectonic contact between the Metaserpentinites and the overlying Metapelites and metasandstones makes it difficult to define their original relationships. In fact, the former could be considered as the basal stratigraphic unit of the original Ligurian succession of the Montecristo Island as it

occurs in the Ligurian successions of the island of Elba and of Southern Tuscany (Nirta et al., 2005; Principi et al., 2015; Pandeli et al., 2018). In this case the shearing processes, that occurred during the Apenninic tectogenesis and during the emplacement of the pluton (see later), delaminated most of the formations of the original Ligurian succession. Another hypothesis is to consider these meta-ophiolitic rocks as an olistolith originally present inside the Ligurian, Early-Late Cretaceous shaly formations, i.e., in the Palombini shales and in Val Lavagna Shales (see Abbate et al., 1970; Nirta et al., 2005 and references therein).

Contact metamorphism zonation

The petrographic and X-ray diffraction (XRD) mineral-ogical analyses carried out on hornfels samples collected in the different outcrops allow to define the metamorphic grade they acquired during contact metamorphism.

The metamorphic zonation of the aureole of the Montecristo pluton was defined on the basis of the hornfels facies (e.g.,, Winkler, 1979, Turner, 1981; Kerrick, 1991; Bucher and Frey, 1994; Philpotts and Ague, 2009; Bucher and Grapes, 2011; Winter, 2014), i.e., the albite-epidote facies (low grade), the hornblende facies (medium grade) and the pyroxene facies (high grade). Pressure values are considered approximately 0.2 GPa (4-6 km) as established by different Authors (Dini et al., 2002; Rocchi et al., 2003b, 2010; Westerman et al. 2004; Rossetti et al., 2007; Caggianelli et al., 2018) for the Mt. Capanne pluton in the Elba island that was emplaced at the same structural level within the highest part of the Apenninic nappe stack (i.e., in the Ligurian Nappes).

Metagabbros

Metagabbros are characterized by the mineral association Pl (20-45 mol% An) + Tr + Act ± Qtz ± Bt (± Cpx). Porphyroclasts of Aug frequently show Act rims and Pl are locally partially albitized. Given the lack of Hbl, the stabil-

ity of Tr + Act association suggests temperature lower than 500°C (albite-epidote facies or albite-actinolite-chlorite zone and, locally, the possible transition to hornblende facies in Winkler 1979; Winter 2014).

Metaserpentinites

They are essentially formed by Tr that include more or less amphibolitized relics of Di. The absence of Srp (transition Srp to Tr at about 450°C, Kerrick, 1991) and the local presence of Hbl±Grt (cfr. Mittempergher, 1954) suggest that these associations are attributable to the transition between albite-epidote to hornblende facies with temperature of at least 500-530°C (Kerrick, 1991; Philpotts and Ague, 2009).

Metapelites and metasandstones

They are characterized by different mineral associations:

1) Bt + Ms + Qtz + Pl (15-38 mol% An) ± Ep ± Spn

This assemblage is present in Outcrop 6 and, locally, in Outcrops 3, 4 and 5. This syn-kinematic mineral assemblage indicates the higher part of the albite-epidote facies (Bucher and Grapes, 2011; Winter, 2014) and T max of 530°C given the lack of Crd and And (Bucher & Frey, 1994). In Outcrop 6, hydrothermal veins are frequent and represented by Ep + Fe-Ax, Qtz + Ep, Qtz + Adl ± Cal and Qtz + Chl + Cal, suggesting temperatures > 250°C during their filling (cfr. Bertini et al., 1985; Ruggieri et al., 2006).

2) Bt + Ms + Qtz ± Pl± Cpx ± Spn ; Grs-Adr ± Tr and Grt ± Cpx (Di-Hd) ± Pl ± Tr ± Bt ± Qtz ± Ms (in the skarn levels)

These associations were defined in the lower part of the Outcrops 3,4 and 5, where the Grt-rich skarn levels (Grt ± Cpx ± Ep ± Pl 56-68 mol% An) locally occur within the metasilici-clastic rocks whose foliation is made up of Bt + Ms + Qtz ± Pl (47-60 mol% An) ± Cpx. The skarn levels were likely originated through decarbonation reactions of limestone-marly intercalations, driven by the local upflowing hot magmatic
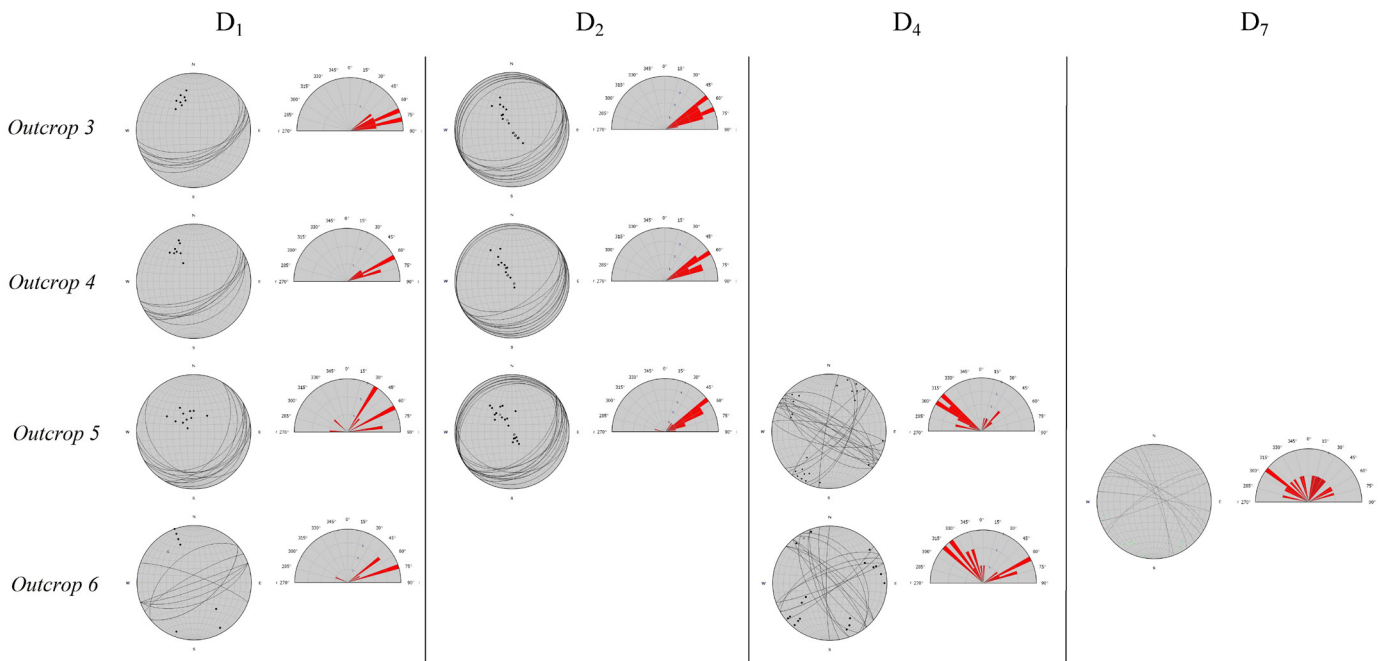

Fig. 12 - Stereographic nets (poles and cyclographic plots; Schmidt, lower hemisphere) and rose diagrams of the structural elements measured in different outcrops of the Metapelites and metasandstones (see locations in Fig. 2b). D_1 and D_2 ductile events (S_1 and S_2 foliations); D_4 (attitude of the high-angle joints) and D_7 (attitude of transtensional faults) brittle events.

fluids, as evident in the hornfels of the Mt. Capanne pluton (Rossetti et al., 2007; Pandeli et al., 2018). These processes allowed ion mobilization (especially Ca, Fe and Al) and formation of Grs-Adr (see also Innocenti et al., 1997).

The mineral assemblage 2) of the skarns can be attributed to a medium-grade metamorphic imprint as defined in Pandeli et al. (2018), with T around 600°C.

The medium- to high-grade mineral associations of the Qtz + Px or Di + Pl (53-75 mol% An) ± Grt ± Wo (as salband) veins, that locally occur in the metasiliciclastic rocks, are also likely related to the circulation and ascent of hot fluids in joints originated by hydrofracturation (see Rossetti et al., 2007; Pandeli et al., 2018).

These metamorphic mineral associations can grow both syn-kinematic within the schistosity planes (see Cpx in Fig. 7j) as well as static (Grt in Fig. 7l) over the lithologic anisotropies and foliations. Such evolution may be attributed to at least two distinct HT recrystallyzation which occurred during the "forced" emplacement of the hot pluton (see later) and the associated circulation of magmatic fluids in the fractured host rocks.

The lack of high grade metamorphic associations and the ubiquitous tectonic contacts of the hornfels with the magmatic bodies allows us to interpret the outcrops of the Montecristo metamorphic aureole as "roof pendants", in agreement with Innocenti et al. (1997).

In some outcrops (e.g., 4 and 5), an evident upward decrease of the metamorphic grade conditions (to very low grade) can be observed within a few tens of meters inside the hornfels successions. This suggests a significant reduced thickness of the contact aureole compared to that of the other plutons in the Tuscan Archipelago and in the Tuscan hinterland. For example, Pandeli et al. (2018) defined an at least 200 m-thick aureole (up to 400 m for Bouillin, 1983) for the Mt. Capanne pluton, but the volume of this latter granitoid can be estimated as 3-4 time greater than the Montecristo one. Considering also the tectonic elision of the middle-lower part of the Montecristo aureole, we suggest a possible total thickness of about 60-100 m.

Deformation evolution

A complex deformation history, related to the intrusion and exhumation of the magmatic body, characterizes the hornfels rocks of Montecristo island. In spite of the small extent and scattering of the outcrops of contact aureole, the present study allowed us to define several deformation stages in the magmatic rocks and in the Cala S. Maria-Cala dei Ladri Unit (see Structural data) through crosscutting criteria between structures (joints, faults, mylonites, protomylonites and pseudotachylites) and dikes/ hydrothermal veins. In particular, magmatic bodies and hornfels suffered ductile and subsequent brittle events that are discussed below in time sequence (see Figs. 4, 13 and Table 4 for the synthesis of structural evolution; M events in the magmatic bodies, D events in the Metapelites and metasandstones):

M_1mf (= magmatic flow) - It is related to the local magmatic flow present inside the melt of the monzogranitic plutonic body.

D_1 - Recrystallization and development of the main schistosity S_1 in the hornfels (generally parallel to the pluton boundary and to the lithological partitions). This foliation was formed during the emplacement of the pluton because S_1 is made by the low- to medium-grade hornfels facies minerals that are also locally present as static blasts (e.g., Px, Grt). This

indicates that the dynamic and static recrystallization of the host rocks are related to magmatic heat transfer. Micro- and meso-structures also suggest that deformation and recrystallization of the host rocks was likely accompanied by a flattening processes connected to the "forced" emplacement of the pluton, similarly to the Mt. Capanne pluton in the Elba Island (Daniel and Jolivet, 1995; Pandeli et al., 2018). Kinematic indicators (book-shelf, σ 1 porphyroclasts, etc.) suggest a top-to-the-south shearing (see Figs. 7j and 11c) for the metasedimentary rocks of Outcrops 2, 3, 4, 5 and 6, consistent with the shape of the southern part of the pluton. The presence of local Cpx and Pl porphyroclasts and glomeroporphyroclasts sheared along S_1, likely suggests a progressive deformation during D_1, that also produced the boudinage of the Grt-rich metasomatic levels. Hydrofracturing of the rocks, along or at different angles respect to S_1, also occurred , due to the ascent of supercritical hot magmatic fluids. They deposited HT minerals in veins that were then deformed by D_2 (Fig. 7h and i). Ductile shearing structures are also present in the Metagabbros (e.g. mylonitic horizons) and in the Metaserpentinites.

M_1my (= mylonitic event) - caused the local NW-SE-striking mylonitic shearing within the granitoid (e.g., in the Cale Gemelle area) during the first stages of its cooling and exhumation. This event can be considered likely coeval with at least a part of D_1 affecting the Cala S. Maria-Cala dei Ladri Unit.

D_2 - This low-grade metamorphic folding, generally characterized by close to tight folds with zonal crenulation cleavages, deforms S_1 foliation with a tectonic transport toward SE. Higher ductile conditions were defined in the lower part of the outcrops by the appearance of discrete-type crenulation cleavages (S_2 =Bt ± Ms ± Fe Ox/Hydrox) associated with isoclinal F2 folds (Fig. 7i). F2 axes and S_1 foliations are mainly sub-parallel to top surface of the granitoid body, which is consistent with the pluton emplacement, similarly to the aureole of Mt. Capanne (see Pandeli at al., 2018).

In particular, D_2 deformations can be associated to the exhumation of the partially cooled pluton that allowed formation of ductile detachments and radial sliding of the overlying hornfels.

M_2-M_3 - These events are the first stages of fracturing of the pluton during cooling. In particular, the subsequent joint systems, characterized by different orientations, were filled by the Aplitic dikes and the Qtz and Tur veins dikes, respectively. These two dikes/veins systems are never present in the hornfels and stop at the top of the underlying pluton. So they were likely originated when the hornfels were still in a ductile regime whereas the pluton reached the brittle regime (see also Spiess et al., 2021), but anyway before the final brittle emplacement of the hornfels plates on the granitoid (D_3 event).

D_3 - The progressive exhumation of the almost cooled magmatic body and of the host rocks allows the development of brittle detachments marked by basal cataclasites at the contact between the different hornfels bodies with the underlying granitoid. Tectonic laminations may occur also within the original recrystallized Ligurian successions during this event (Fig. 4) that allowed the final sliding and emplacement of the "roof pendant" bodies.

M_4-D_4 - Mostly unfilled, sub-vertical NW-SE and NE-SW jointing cut both the hornfels and the underlying magmatic rocks. They are likely related to the prosecution of the unroofing and of the further cooling of the pluton. Some hydrothermal activity was still present.
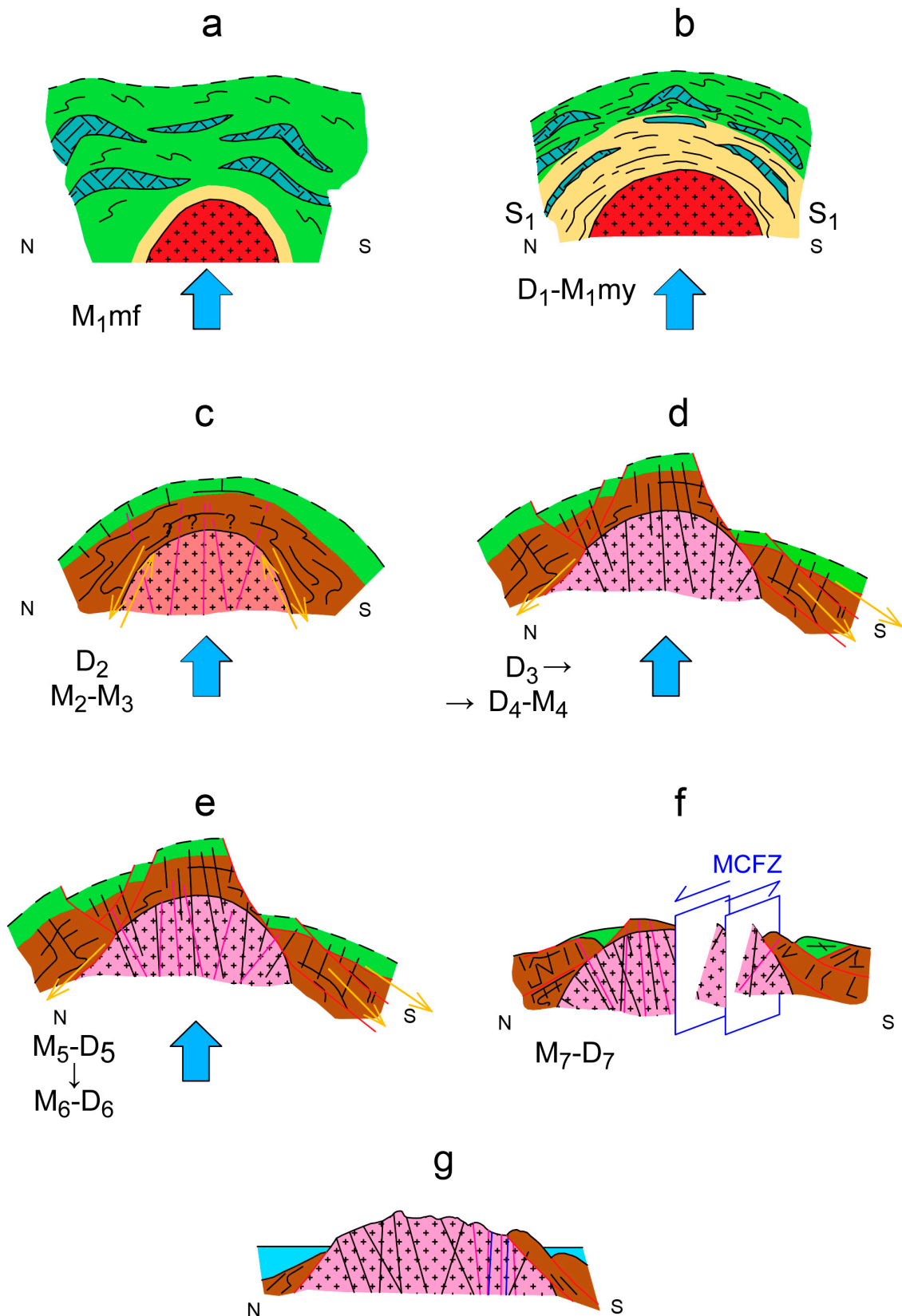
Fig. 13 - Sketch of the geological evolution of the Montecristo island. a) Intrusion of the Messinian monzogranitic pluton (hot = dark red) within the Ligurian successions and beginning of their recrystallization, ballooning of the pluton and magmatic flow (M_1mf); b) D_1 producing S_1 (through flattening process) and contact metamorphism in the Cala S. Maria-Cala dei Ladri Unit host rocks, mylonitic shearing in the granitoid (M_1my); c) Uplift of the partially cooled (light red) pluton, ductile detachments and folding of the host rocks (D_2), intrusion of the Aplitic dikes (M_2) and the Qtz and Tur veins (M_3) in the granitoid; d) Further cooling and exhumation of the pluton (pink) triggers brittle detachments and delaminations of the host rocks giving rise to the "roof pendant" bodies (D_3) followed by sub-vertical fracturing of both granitoids and roof pendants (M_4-D_4); e) Intrusion of the Tur-bearing porphyritic dikes and veins in the Monzogranite and in the Cala S. Maria-Cala dei Ladri Unit host rocks (M_5-D_5) and of the Porphyritic dikes (M_6-D_6) subsequently; f) Sinistral shearing event (MCFZ= Cala Maestra-Cala Corfù Fracture Zone) in the southern part of the isle (M_7-D_7) likely due to reactivation of regional stress; g) Present situation.

M₅-D₅ - This magmatic-tectonic phase is characterized by NNW-SSE and NW-SE to ENE-WSW fracturing and intrusion of the TPDnb and TPDb respectively in both the cold granitoid and overlying "roof pendant" bodies.

M₆-D₆ - A new magmatic-tectonic pulse generates a main WNW-ESE fracturing and intrusion of the Porphyritic dikes, cutting hornfels and previous magmatic bodies. According to Innocenti et al. (1997), the Porphyritic dikes derive from a different magmatic source respect to the Montecristo pluton.

M₇-D₇ - A final shear event, that was presumably influenced by the regional stress, affected the southern part of the island forming the wide Cala Maestra-Cala Corfù Fracture Zone , likely by re-using part of the D₄ joints. The presence of both sinistral and dextral transcurrent structures and associated protomylonites and pseudotachylites points to a ENE-WSW σ1 orientation and defines an overall sinistral Riedel system for the Cala Maestra-Cala Corfù Fracture Zone and surrounding areas as shown by the reconstruction of the paleo-stress field obtained from the inversion of fault data (see Fig. 14).

The metamorphic deformative evolution of the aureole of the Montecristo granitoid is similar to that of Mt. Capanne pluton also because of their intrusion in the superficial structural levels of the orogenic pile, i.e., the Ligurian successions. Anyway, D₁ represents the ductile contact metamorphic peak in the Montecristo aureole that corresponds to main D₂ deformation and recrystallization event in the western Elba host rocks where a previous syn-metamorphic isoclinal folding was also defined by Pandeli et al. (2018). The absence of the latter event in the Montecristo aureole can be probably related to a little different deformation history of the host rocks or to the strong transposition of the eventual previous structures that occurred during the D₁ event in the Cala S. Maria-Cala dei Ladri Unit.

The last deformation event (D₇) defined in the Island of Montecristo is characterized by an overall NW-SE sinistral transtensional shearing due to the activation of the extensive Cala Maestra-Cala Corfù Fracture Zone in the southern part of the isle. The occurrence of Neogene-Quaternary strike-slip tectonics in the Northern Apennines was pointed out by
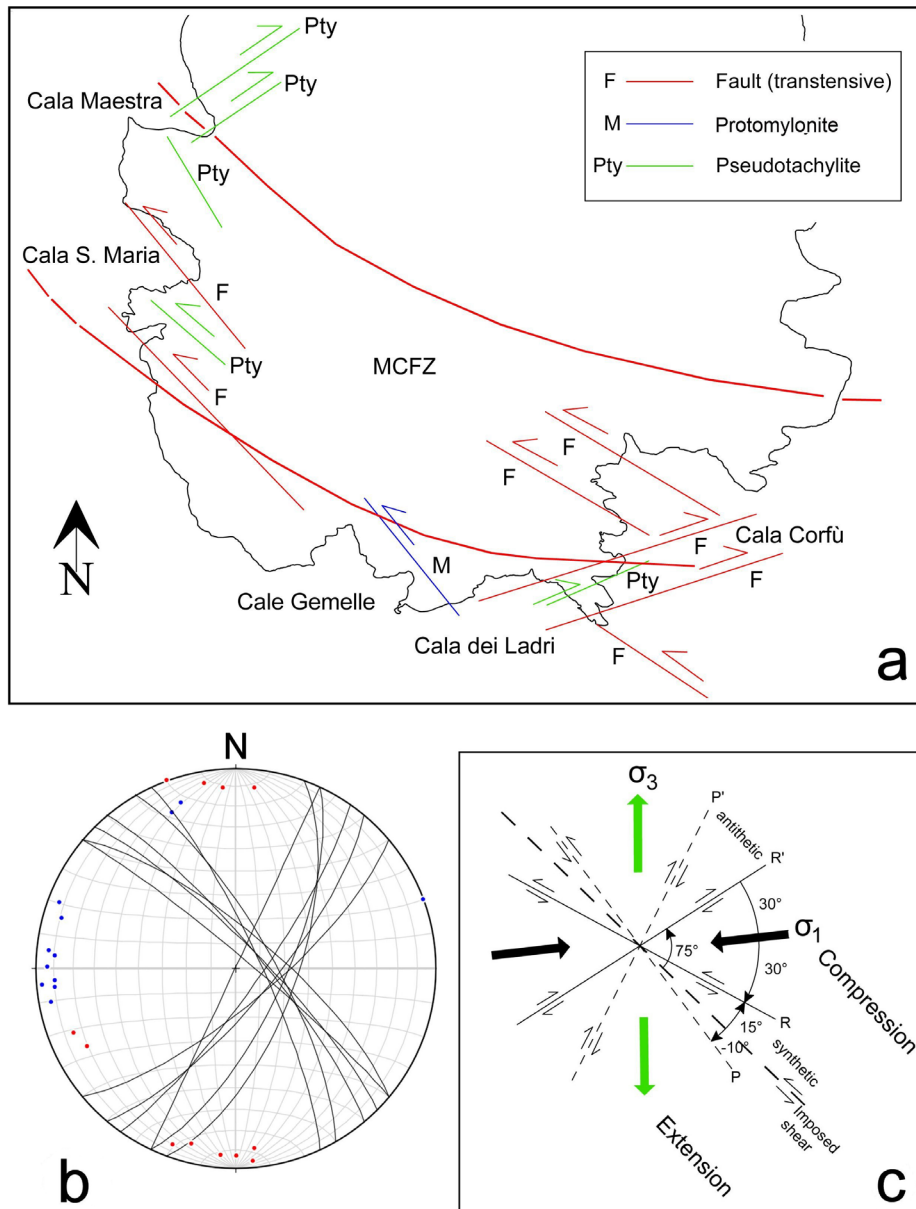

Fig. 14 - a) Structural sketch of the Cala Maestra-Cala Corfù Fracture Zone shear zone (MCFZ) in the southern part of the Montecristo Island with the main structural lineaments: F = transtensive fault, M = pseudomylonite, Pty = pseudotachylite; b) Stereonet of the paleo-stress field obtained from the inversion of M₇ and D₇ data of the brittle and brittle-ductile shear lineaments using FAULTKIN 8 program by Allmendinger et al. (2012); blue points = shortening (σ1) and red points = extension (σ3). c) Reconstruction of the stress field that points to a ENE-WSW σ1 orientation and defines an overall sinistral Riedel system for Cala Maestra-Cala Corfù Fracture Zone and surrounding areas.

Elter et al. (2012) through geological and seismic data. They identified NE-SW-directed transtensive and overall NW-SE sinistral transpressive lineaments in the Tuscan hinterland both coexisting in a Riedel shear model and related them to the push of the African plate against Europe. Moreover, Elter & Sandrelli (1995) associated the regional alignments of the coeval granitoid bodies to transcurrent NW-SE structural lineaments in Southern Tuscany and Tuscan Archipelago.

Also other Authors hypothesized the presence of transfer and transcurrent structures in the Tuscan Archipelago and hinterland (Bartole, 1994; Cornamusini and Pascucci, 2014) (see Fig. 1) and particularly in the Elba Island where the emplacement of the plutonic bodies and dike swarms seems to be driven by an about E-W – trending sinistral strike slip lineament (Bouillin et al., 1993) or by a NE-SW dextral shearing ("Western Elba Transfer Zone" in Dini et al., 2008). Finally, Liotta et al. (2015) and Spiess et al. (2021) documented ductile deformation occurred during the fast exhumation of the Late Miocene Porto Azzurro pluton emplaced in a NE-striking, extensional to transcurrent tectonic setting in SE Elba Island (i.e., the "Capoliveri-Porto Azzurro shear zone").

The similar shear orientation of the mylonites in the Monzogranite (M_1my event; Fig. 8) with the final transtensive M_7-D_7 shearing in Cala Maestra-Cala Corfù Fracture Zone suggest a long living regional stress field in the southern part of the Montecristo island that possibly was already active during the intrusion of the pluton.

CONCLUSIONS

The mapping and structural-petrographic study of the hornfels of the Montecristo pluton (here grouped into the informal Cala S. Maria-Cala dei Ladri Unit) allowed not only to define their detailed lithological and compositional features, but also their metamorphic-structural evolution during the intrusion and unroofing of the granitoid. The following results can be pointed out:

1) Most of the relict outcrops of the contact metamorphic aureole in the southern part of the island are made up of alternating metapelites and quartzitic metasandstones with minor metacarbonate intercalations transformed in Grt-rich skarn levels (Metapelites and metasandstones unit). Two metaserpentinite bodies were distinguished for the first time in the SW areas, whereas only metagabbros are present in the metaophiolitic hornfels in the southern promontory of Cala S. Maria. All these lithotypes can be referred to the Internal Ligurian successions. In particular,. the protholith of the Metapelites and metasandstones unit can be correlated with the Quartzarenitic Member of the Early Cretaceous Palombini Shales and/or with part of the Early-Late Cretaceous Lavagna Shales.

2) The contact metamorphism in the Cala S. Maria-Cala dei Ladri Unit generally varies from very low to the medium grade (hornblende facies). Only the Grt-rich skarn bodies and the HT mineral associations present in veins, testifying higher metamorphic conditions due to the local ascent of very hot metasomatic fluids from the pluton and hydrofracturing phenomena within the aureole. Since all the hornfels bodies are in tectonic contact with the underlying Monzogranite, the former may be considered as "roof pendants", whereas the higher grade hornfels were probably tectonically removed. Anyway, a relatively small thickness of the Montecristo contact aureole (probably about 60-100 m-thick) can be hypothesized.

3) The metamorphic and deformation evolution of the hornfels is very complex and includes seven events that can be possibly referred to a continuum tectono-magmatic evolution.

In particular, ductile deformations occurred in both magmatic body (i.e., mylonitic horizons, M_1my event) and in host rocks (D_1 and D_2 events). Particularly, D_1 is related to the forced intrusion of the hot magmatic body that produced the main metamorphic foliation S_1 made up of contact metamorphic minerals through flattening processes. The filling of hydrofractures in the hornfels with HT minerals also occurred at the end of this stage. The following low grade metamorphic D_2 folding with associated crenulations occurred during the cooling of the system. The ductile detachments in the covers of the pluton began during the ductile D_2 and continued during the brittle D_3 when the "roof pendants" reached the present position on the granitoid body through their basal cataclastic horizons. Before D_3, the Aplitic dikes and the Qtz and Tur veins intruded different joint systems (M_2 and M_3) present only within the plutonic body during its cooling. Then, the ascent of the cold plutonic body was associated to the formation of a subvertical, mostly unfilled joints in both pluton (M_4) and overlying hornfels (D_4). The D_4 joints were then cut by other two jointing events (M_5-D_5) and (M_6-D_6) filled by PTD and by the Porphyritic dikes, respectively . Finally, the southern part of the island was affected by a wide NW-SE striking, transtensive sinistral shearing (Cala Maestra-Cala Corfù Fracture Zone) (M_7-D_7) with an about ENE-WSW σ 1, likely due to reactivation of regional stress.

4) MCFZ represent one of the few outcropping witnesses of transcurrent and transfer structures in the Tuscan Archipelago that were used for the intrusion and ascent of the different magmatic bodies (e.g., Bouillin et al., 1993; Dini et al., 2008; Liotta et al., 2015; Spiess et al., 2021 in the Elba Island). The similar shear orientation of the M_1my mylonites in the Monzogranite with the final transtensive M_7-D_7 shearing in the main Cala Maestra-Cala Corfù Fracture Zone suggests that the transcurrent tectonics was active for a long time in the Montecristo island, at least during the intrusion and uplift of the pluton.

REFERENCES

Abbate E., Bortolotti V., Passerini P. and Sagri M., 1970. Introduction to the geology of the Northern Apennines. Sedim. Geol., 4(3-4): 207-249.

Allmendinger R.W., Cardozo N.C. and Fisher D., 2012. Structural geology algorithms: Vectors and Tensors. Cambridge, Univ. Press, 289 pp.

Bartole R., 1995. The North Tyrrhenian - Northern Apennines post-collisional system: constraints for a geodynamic model. Terra Nova, 7 (1): 7-30.

Bartole R., Torell i L., Mattei G., Peis D. and Brancolini G., 1991. Assetto stratigrafico-strutturale del Tirreno settentrionale: stato dell'arte. Studi Geol. Camerti, Vol. Spec. (1991/1): 115-140.

Bertini G., Gianelli G., Pandeli E. and Puxeddu M., 1985. Distribution of hydrothermal minerals in the Larderello-Travale and Mt. Amiata geothermal fields (Italy). Trans. 1985 Intern. Symp. Geothermal energy held in Kailua-Kona (Hawaii), August 1985. Geothermal Resources Council, Davis (USA), 9 (1): 261-266.

Bianco C., Brogi A., Caggianelli A., Giorgetti G., Liotta D. and Meccheri M., 2015. HP-LT metamorphism in Elba Island: implications for the geodynamic evolution of the inner Northern Apennines (Italy). J. Geodyn. 91: 13-25.

Boni A., Braga G., Conti S., Gelati R., Marchetti G. and Passeri, L.D., 1969. Note illustrative della Carta Geologica d'Italia alla scala di 1: 100.000, Foglio 83 «Rapallo» e Foglio 94 «Chiavari». Serv. Geol. d'It. (Min. Ind.), Roma, 89 pp.

Bortolotti V., Fazzuoli M., Pandeli E., Principi G., Babbini A. and Corti S., 2001. Geology of Central and Eastern Elba Island, Italy. Ofioliti, 26 (2a): 97-151.

Bouillin J.P., 1983. Exemples de déformations locales liées à la mise en place de granitoïdes alpins dans des conditions distensives: l'Ile d'Elbe (Italie) et le Cap Bougaroun (Algérie). Rev. Géol. Dyn. Géogr. Phys., 24: 101-116.

Bouillin J.-P., Bouchez J.-L., Lespinasse P. and Pecher A., 1993. Granite emplacement in an extensional setting: an AMS study of the magmatic structures of Monte Capanne (Elba Island, Italy). Earth Planet. Sci. Lett., 118: 263-279.

Bucher K. and Frey M., 1994. Petrogenesis of metamorphic rocks 6th ed., Springer Ed. 318 pp.

Bucher K. and Grapes R., 2011. Petrogenesis of metamorphic rocks 8th ed., Springer Ed. 428pp.

Caggianelli A., Zucchi M., Bianco C., Brogi A. and Liotta D., 2018. Estimating P-T metamorphic conditions on the roof of a hidden granitic pluton: an example from the Mt. Calamita promontory (Elba Island, Italy). It. J. Geosci., 137 (2): 238-253.

Carmignani L., Decandia F.A., Disperati L., Fantozzi P.L., Kligfield R., Lazzarotto A. and Meccheri M., 2001. Inner Northern Apennines. In G.B. Vai and I.P. Martini (Eds.), Anatomy of an orogen: The Apennines and adjacent Mediterranean basins. Springer Sci. and Business Media, p. 197-214.

Conticelli S., Boari E., Burlamacchi L., Cifelli F., Moscardi F., Laurenzi M. A. and Manetti P., 2015. Geochemistry and Sr-Nd-Pb isotopes of Monte Amiata Volcano, Central Italy: evidence for magma mixing between high-K calc-alkaline and leucititic mantle-derived magmas. It. J. Geosci., 134 (2): 266-290.

Cornamusini G. and Pascucci V., 2014. Sedimentation in the Northern Apennines-Corsica tectonic knot (Northern Tyrrhenian Sea, Central Mediterranean): offshore drilling data from the Elba-Pianosa Ridge. Int. J. Earth Sci (Geol Rundsch), 103 (3): 821-842.

D'Achiardi A., 1872/73. Mineralogia della Toscana. Tipografia Nistri, Pisa, 2 vol., 678 pp.

Daniel J.M. and Jolivet L., 1995. Detachment faults and pluton emplacement: Elba Island (Tyrrhenian Sea). Bull. Soc. Géol. Fr., 166: 341-354.

Davis R.H. and Reynolds S.J., 1996. Structural geology of rocks and Regions. Wiley and Sons Ed., 776 pp. .

Dini A., Innocenti F., Rocchi S., Tonarini S. and Westerman D.S., 2002. The magmatic evolution of the late Miocene laccolith-pluton-dyke granitic complex of Elba Island, Italy. Geol. Mag., 139: 257-279.

Dini A., Westerman D.S., Innocenti F. and Rocchi S., 2008. Magma emplacement in a transfer zone: the Miocene mafic Orano dyke swarm of Elba Island, Tuscany, Italy. Geol. Soc. London, Spec. Publ., 302 (1): 131-148.

Doglioni C., Gueguen E., Harabaglia P. and Mongelli F., 1999. On the origin of west-directed subduction zones and applications to the western Mediterranean. Geol. Soc. London Spec. Publ., 156 (1): 541-561.

Elter F.M. and Pandeli E., 2002. The HP-LP meta-ophiolitic unit and Verrucano of the Cala Grande Area in the Argentario Promontory (Southern Tuscany, Italy): structural-metamorphic evolution and regional considerations. Ofioliti. 27: 91-102.

Elter F.M. and Sandrelli F., 1995. La Fase Post Nappe nella Toscana Meridionale: considerazioni sull'evoluzione dell'Appennino Settentrionale. Atti Ticin. Sci. Terra, Pavia, 37: 173-193.

Elter F. M., Elter P., Eva C., Eva E., Kraus R.K., Padovano M. and Solarino S., 2012. An alternative model for the recent evolution of the Northern-Central Apennines (Italy). J. Geodyn., 54: 55-63.

Ferrara G. and Tonarini S., 1985. Radiometric geochronology in Tuscany: Results and problems. Rend. Soc. It. Miner. Petrol., 40: 111-124.

Fossen H., 2010. Structural geology. Cambridge Univ. Press, 463 pp.

Garfagnoli F., Menna F., Pandeli E. and Principi G., 2005. The Porto Azzurro Unit (Mt. Calamita Promontory, southeastern Elba Island, Tuscany): stratigraphic, tectonic and metamorphic evolution. Boll. Soc. Geol. It., Vol. Spec., 3: 119-138.

Giuli G., 1843. Saggio statistico di mineralogia utile della Toscana. Parte IV. Nuovi Ann. Sci. Nat. Bologna, 5, 10, 273-301.

Innocenti F., Serri G., Ferrara G., Manetti G. and Tonarini S.. 1992. Genesis and classification of the rocks of the Tuscan Magmatic Province: thirty years after Marinelli's model. Acta Vulcan., 2: 247-265.

Innocenti F., Westerman D.S., Rocchi S., Tonarini S., 1997. The Montecristo Monzogranite (Northern Tyrrhenian Sea Italy): a collisional pluton in an extensional setting. Geol. J., 32, 131-151.

Jervis G., 1874. I tesori sotterranei dell'Italia. Vol. 2: Regione dell'Appennino e vulcani attivi e spenti dipendentivi. Ed. Loescher, Torino, 624 pp.

Jolivet L., Faccenna C., Goffé B., Mattei M., Rossetti F., Brunet C. and Parra T., 1998. Midcrustal shear zones in postorogenic extension: example from the northern Tyrrhenian Sea. J. Geophys. Res.: Solid Earth, 103 (B6): 12123-12160.

Kerrick D.M., 1991. Overview of contact metamorphism. Rev. Miner. Geochem., 26 (1): 1-12.

Lazzarotto A., 1967. Geologia della zona compresa fra l'alta Valle del Fiume Cornia ed il Torrente Pavone (Prov. di Pisa e Grosseto). Mem. Soc. Geol. It., 6: 151-197.

Liotta D., Brogi A., Meccheri M. Dini A., Bianco C. and Ruggieri G., 2015. Coexistence of low-angle normal and high-angle strike- to oblique-slip faults during Late Miocene mineralization in eastern Elba Island (Italy). Tectonophysics, 660: 17-34.

Marinelli G., 1967. Genòse des magmas du vulcanisme plio-quaternaire des Apennins. Geol. Runds., 57: 127-141. The deformation history of an accreted ophiolite sequence: the Internal Ligurid units (Northern Apennines, Italy), Geodyn. Acta, 9 (1): 13-29

Marroni M., Bortolotti V., Cortesogno L., Gaggero L., Lahondere D., Molli G., Montanini A., Pandolfi L., Principi G., Rossi P., Saccani E., Treves B. and Tribuzio R., 2004. Northern Apennine and Corsican ophiolites: the oceanic lithosphere of the Ligure-Piemontese basin and its transition to the Adria continental margin (Italy). In: L. Guerrieri, I. Rischia and L. Serva (Eds.), Excursion Guidebook 32nd Intern. Geol. Congr. ITALIA 2004., Vol. 4 (P14 - P36), P 27 Post-Congress Field Trip Guide. Apat, Roma: 52 pp.

Martini I. P. and Sagri M., 1993. Tectono-sedimentary characteristics of Late Miocene-Quaternary extensional basins of the Northern Apennines, Italy. Earth-Sci Rev., 34 (3): 197-233.

Mauffret A. and Contrucci I., 1999. Crustal structure of the north Tyrrhenian Sea: first result of the multichannel seismic LISA cruise. In: B. Durand, L. Jolivet, F. Horvat and M. Seranne (Eds.), The Mediterranean Basins: Tertiary extension within the Alpine Orogen, Geol. Soc. London Spec. Publ., 156: 169-193.

Millosevich, F., 1912. Zeunerite e altri minerali dell'isola di Montecristo. Atti R. Accad. Naz. Lincei, Rend. Cl. Sci. Fis. Mat. Nat., Ser. 5, 21: 594-597.

Mittempergher M. 1954. L'isola di Montecristo. Ricerche petrologiche e psammografiche. Atti Soc. Tosc. Sci. Nat., Mem., Serie A, 61: 167-218.

Mukherjee S., 2014. Atlas of shear zone structures in Meso-scale. Springer Ed., 124pp.

Nirta G., Pandeli E., Principi G., Bertini G. and Cipriani N., 2005. The Ligurian units of Southern Tuscany. Boll. Soc. Geol. It., Vol. Spec., 3: 29-54.

Orti L., Morelli M., Pandeli E. and Principi G., 2002. New geological data from Gorgona Island (Northern Tyrrhenian Sea). Ofioliti, 27: 133-144.

Palache C., Berman H. and Frondel C., 1951. The System of Mineralogy of James Dwight Dana and Edward Salisbury Dana, Yale University 1837-1892. John Wiley and Sons, Inc., New York, 7th Ed., Vol. 2 , 1124 pp.

Pandeli E., Puxeddu M. and Ruggieri G., 2001. The metasiliciclastic-carbonate sequence of the Acquadolce Unit (Eastern Elba Island): new petrographic data and paleogeographic interpretation. Ofioliti,26 (2a): 207-218.

Pandeli E., Bertini G., Castellucci P., Morelli M. and Monechi S., 2005. The sub-Ligurian and Ligurian units of the Mt. Amiata geothermal region (south-eastern Tuscany): new stratigraphic and tectonic data and insights into their relationships with the Tuscan Nappe. In: A. Brogi, A. Lazzarotto and D. Liotta (Eds.), Results of the CROP 18 Project. Boll. Soc. Geol. It., Vol. Spec., 3: 55-71.

Pandeli E., Giusti R., Elter F.M., Orlando A. and Orti L., 2018. Structural setting and metamorphic evolution of a contact aureole: the example of the Mt. Capanne pluton (Elba Island, Tuscany, Italy). Ofioliti, 43 (1): 41-73.

Pareto L., 1844. Sulla costituzione geologica delle isole di Pianosa, Giglio, Giannutri, Montecristo, e Formiche di Grosseto. In: Atti della quarta unione degli scienziati italiani tenuta in Lucca nel settembre 1843. Sezione di geologia, mineralogia, e geografia. Atti del dì 27 Settembre 1841. Tip. Giusti, Lucca, p. 269-272.

Passchier W. and Trouw R.A.J., 1996. Micro-tectonics. Springer Ed., 289 pp..

Patacca E., Sartori R. and Scandone P., 1993. Tyrrhenian Basin and Apennines. Kinematic evolution and related dynamic constraints. In: E. Boschi, E. Mantovani and A. Morelli (Eds), Recent evolution and seismicity of the Mediterranean Region. NATO ASI Series (Series C: Math. Phys. Sci.), 402: 161-171. Springer, Dordrecht.

Peccerillo A., 2005. Plio-Quaternary Volcanism in Italy. Ed. Springer-Verlag Berlin Heidelberg XIV, 365.

Philpotts A., and Ague J., 2009. Principles of igneous and metamorphic petrology. Cambridge Univ. Press. 684 pp.

Poli G. and Peccerillo, A., 2016. The Upper Miocene magmatism of the Island of Elba (Central Italy): compositional characteristics, petrogenesis and implications for the origin of the Tuscany Magmatic Province. Miner. Petrol., 110: 1-25.

Poli G., Manetti P. and Tommasini S., 1989. A petrological review on Miocene-Pliocene intrusive rocks from southern Tuscany and Tyrrhenian Sea (Italy). Per. Miner., 58: 109-126.

Principi G., Bortolotti V., Pandeli E., Fanucci F., Chiari M., Dini A., Fazzuoli M., Menna F., Morelli D., Moretti S., Nirta G. and Reale V., 2015. Note illustrative della Carta Geologica d'Italia alla scala 1:50000, Foglio 316, 317, 328, 329, Isola d'Elba. 265 pp. Delivered to Servizio Geologico d'Italia, Roma

Rocchi S., Dini A., Innocenti F., Tonarini S. and Westerman D. S. (2003b). Elba Island: intrusive magmatism. Per. Miner., 72 (2): 73-104.

Rocchi S., Westerman D.S., Dini A. and Farina F., 2010. Intrusive sheets and sheeted intrusions at Elba Island (Italy). Geosphere, 6: 225-236

Rocchi S., Westerman D.S. and Innocen ti F., 2003a. Montecristo Island: intrusive magmatism. Per. Miner., 72: 105-118.

Rossetti F., Tecce F., Billi A. and Brilli M., 2007. Patterns of fluid flow in the contact aureole of the Late Miocene Monte Capanne pluton (Elba Island, Italy): the role of structures and rheology. Contrib. Miner. Petrol., 153: 743-760.

Roster G., 1876. Note mineralogiche su l'Isola d'Elba. Parte prima - anno 1875. Boll. R. Comitato Geol. d'It., 7, 7-8: 297-323.

Ruggieri G., Petrone C.M., Gianelli G., Arias A. and Torio Henriquez E., 2006. Hydrothermal alteration in the Berlin geothermal field (El Salvador): new data and discussion on the natural state of the system. Per. Miner., 75 (2-3): 293-312.

Sartori R., Kastens K., Mascle J. and Auroux C., 1989. Drillings of ODP Leg 107 in the Tyrrhenian Sea: tentative basin evolution compared to deformations in the surrounding chains. In: A. Boriani, M. Bonafede, G.B, Piccardo and G.B. Vai (Eds.), The Lithosphere In Italy. Accad. Naz. Lincei, Atti Convegni, 80: 139-156.

Serri G., Innocenti F. and Manetti P., 1993. Geochemical and petrological evidence of the subduction of delaminated Adriatic continental lithosphere in the genesis of the Neogene-Quaternary magmatism of Central Italy. Tectonophysics, 223: 117-147.

Serri G., Innocenti F. and Manetti P., 2001. Magmatism from Mesozoic to Present: petrogenesis, timespace distribution and geodynamic implications. In: G.B. Vai and I.P. Martini (Eds.), Anatomy of an Orogen: The Apennines and Adjacent Mediterranean Basins. Springer Sci. and Business Media, p. 7-104.

Smith W. and Warington J., 1841. Sulla costituzione geologica dell'Isola di Monte Cristo. In: Atti 3ª riunione degli scienziati italiani, Firenze nel settembre 1841. Sezione di geologia, mineralogia, e geografia. Atti del dì 29 Settembre 1841. Tip. Galileiana, Firenze, p. 191-192.

Spiess R. Langone A., Caggianelli A., Stuart FM., Zucchi M., Bianco C., Brogi . and Liotta D., 2021. Unveiling ductile deformation during fast exhumation of a granitic pluton in a transfer zone. J. Struct. Geol., 147: 104326.

Spohn A., 1981. Die ophiolitführenden Gesteine von West-Elba: Stratigraphie, Tektonik, Metamorphose. Berliner Geowiss. Abh. Reihe, A 37, 124 pp.

Trouw R.A.J., Passchier C.W. and Wiersma D.J., 2009. Atlas of mylonites and related microsrtuctures. Springer Ed., 322 pp.

Turner F.J., 1981. Metamorphic petrology - Mineralogical, field and tectonic aspects. 2nd Ed. McGraw-Hill, New York, 524 pp.

Ugolini R., 1909. Rocce di Montecristo. Atti R. Accad. Fisiocritici Siena, 6: 1-16.

Westerman D.S., Dini A., Innocenti F. and Rocchi S., 2004. Rise and fall of a nested Christmas-tree laccolith complex, Elba Island, Italy. In: N. Petford and C. Breitkreutz (Eds.), Physical geology of high-level magmatic systems. Geol. Soc. London Spec. Publ., 234: 195-213.

Whitney D. and Evans B., 2010. Abbreviations for names of rockforming minerals. Am. Miner.. 95: 185-187.

Winkler H.G.F., 1979. Petrogenesis of metamorphic rocks. 5nd Ed.. Springer-Werlag, 348 pp.

Winter J.D., 2014. Principles of igneous and metamorphic petrology. Pearson Education Limited Edinburgh Gate, 2nd Ed., 738 pp.

Zitellini N., Trincardi F., Marani M. and Fabbri A., 1986. Neogene tectonics of the Northern Tyrrhenian sea. Giorn, Geol., 48: 25-40.